T.R.
INONU UNIVERSITY
GRADUATE SCHOOL OF NATURE AND APPLIED SCIENCES

MULTIPLE DETECTION OF SARS- CoV-2 IN POINT-OF-CARE TESTS

MASTER THESIS

ELİF GÜNDÜZ

Department of Molecular Biology and Genetics

Thesis Advisor: Asst. Prof. Dr. Dilek ÇAM DERİN

NOVEMBER 2024

T.R
INONU UNIVERSITY
GRADUATE SCHOOL OF NATURE AND APPLIED SCIENCES

MULTIPLE DETECTION OF SARS- CoV-2 IN POINT-OF-CARE TESTS

MASTER THESIS

Elif GÜNDÜZ
36223623003

Department of Molecular Biology and Genetics

Thesis Advisor: Asst. Prof. Dr. Dilek ÇAM DERİN

NOVEMBER 2024

İNÖNÜ ÜNİVERSİTESİ
FEN BİLİMLERİ ENSTİTÜSÜ MÜDÜRLÜĞÜ

Multiple Detection of SARS-CoV-2 in Point-of-care Tests

Tezi Hazırlayan: Elif GÜNDÜZ
Yüksek Lisans Tezi

ACKNOWLEDGMENTS

I would like to express my sincere gratitude to my advisor, Asst. Prof. Dr. Dilek ÇAM DERİN for her support throughout my master's degree and thesis work. Her extensive knowledge and experience have been an invaluable resource, constantly inspiring me to struggle for excellence. I am truly grateful for her guidance and encouragement which have been instrumental in my academic journey.

I would like to thank Prof. Dr. Barış OTLU and Dr. Elif Seren TANRIVERDİ from Inonu University Faculty of Medicine, Department of Microbiology for their support to our work.

I would like to thank my dear family, who have been a constant source of strength and inspiration for me on this path. I would like to express my gratitude and appreciation to my family for being able to achieve success with their sacrifices, patience, endless love and unwavering belief in me.

WORD OF HONOR

I hereby declare that this master's thesis titled “Multiple Detection of SARS-CoV-2 in Point-of-Care Tests” is entirely my own work, without seeking any assistance that would be contrary to scientific ethics and traditions, and that it adheres to the principles of scientific ethics and honesty, and that all sources I have used are properly cited according to the method and are listed both within the text and in the bibliography and I confirm this with my honor.

Elif GÜNDÜZ

TABLE OF CONTENTS

ACKNOWLEDGMENTS ..... **i**
WORD OF HONOR ..... **ii**
TABLE OF CONTENTS ..... **iii**
LIST OF TABLES ..... **iv**
LIST OF FIGURES ..... **v**
SYMBOLS AND ABBREVIATIONS ..... **vi**
ÖZET ..... **vii**
ABSTRACT ..... **viii**
1. INTRODUCTION **1**
1.1 Coronaviruses 1
1.2 SARS-CoV-2 Structure and Key Proteins 1
1.2.1 Structure of SARS-CoV-2 1
1.2.2 Role of S protein 2
1.2.3 Role of N protein 3
1.3 Diagnostic Methods for SARS-CoV-2 4
1.4 Lateral Flow Assays (LFAs) 7
1.4.1 Principle and mechanism of LFAs 7
1.5 Multiple Detection in LFAs (mLFAs) 8
1.6 Aptamers and Usage in LFAs 9
1.7 The Role of Aptamer Cocktails in mLFAs 11
1.8 Aim of the Study 12
2. MATERIALS AND METHODS **13**
2.1 Reagents and Apparatus 13
2.2 Synthesis of AuNPs 16
2.3 Preparation of AuNP Labeled N-S Aptamers 16
2.4 Preparation of Aptamer Cocktails and Designing of mLFAs Models 16
2.5 Quantitative Color Intensity Analysis 18
2.6 Clinical Sample Preparation for SARS-CoV-2 Detection 18
2.7 Experimental Strategy 18
3. RESULTS AND DISCUSSION **20**
3.1 Synthesis and Characterization of the AuNPs 20
3.2 Effect of the Concentrations of Aptamer Cocktails in mLFAs 21
3.3 Dual-Target Detection of SARS-CoV-2 in Clinical Specimens with mLFAs 22
3.3.1 Model 1 assay performance 24
3.3.2 Model 2 assay performance 27
3.3.3 Model 3 assay performance 31
3.3.4 Sensitivity and specificity of mLFAs 34
4. CONCLUSION **36**
REFERENCES **37**
CURRICULUM VITAE **43**

LIST OF TABLES

Table 2.1 : Aptamer sequences and prepared assay models for the aptamer cocktails-based mLFAs…….14

LIST OF FIGURES

Figure 1.1 : Schematic representation of SARS-CoV-2's genome structure……2
Figure 1.2 : Schematic representation of some SARS-CoV-2 diagnostic methods……6
Figure 1.3 : A schematic illustration of the design and principle of LFAs……8
Figure 1.4 : The interaction between target-aptamer and general scheme of the SELEX method……11
Figure 2.1 : Working principle of aptamer cocktails-based mLFAs without (A) and with the target (B)……17
Figure 2.2 : Overall of the experimental strategies and methods for SARS-CoV-2 detection in mLFAs……19
Figure 3.1 : UV-Vis spectroscopy (A,B) and size measurement of the synthesized AuNPs by STEM (B).. ……21
Figure 3.2 : Binding affinities of the NP and S aptamers to the SARS-CoV-2 on developed by mLFAs…….....22
Figure 3.3 : Comparison of E1 and E2 membrane in mLFAs developed by Model 1……23
Figure 3.4 : Comparison of binding affinities of N and S aptamers on separate strips…...24
Figure 3.5 : SARS-CoV-2 detection in naso/oropharyngeal swabs on mLFAs developed by Model 1……26
Figure 3.6 : Histogram graph generated using ImageJ software for Model 1. ……...27
Figure 3.7 : SARS-CoV-2 detection in naso/oropharyngeal swabs on mLFAs developed by Model 2……29
Figure 3.8 : Histogram graph generated using ImageJ software for Model 2…….30
Figure 3.9 : Design of the developed mLFAs with different aptamer pairs in conjugation and TL immobilization…….31
Figure 3.10 : SARS-CoV-2 detection in naso/oropharyngeal swabs on mLFAs developed by Model 3…….....33

SYMBOLS AND ABBREVIATIONS

LFA : Lateral Flow Assay
mLFA : Multiple Lateral Flow Assay
DNA : Deoxyribonucleic Acid
RNA : Ribonucleic Acid
AuNP : Gold Nanoparticle
N : Nucleocapsid
S : Spike
E : Envelope
M : Membrane
ELISA : Enzyme-Linked Immunosorbent Assay
CLIA : Chemiluminescent Immunoassay
LAMP : Loop-Mediated Isothermal Amplification
RT-PCR : Reverse Transcription Polymerase Chain Reaction
POCT : Point-of-care Test
TL : Test Line
CL : Control Line
TCEP : Tris(2-Carboxyethyl)phosphine
VNAT : Virus Collection Buffer
SSC : Saline-Sodium Citrate
PBS : Phosphate Buffered Saline
STEM : Scanning/Transmission Electron Microscopy
RB : Running Buffer
λ_{max} : Lambda max

ÖZET

Yüksek Lisans Tezi

HASTA BAŞI TESTLERİNDE ÇOKLU SARS-CoV-2 TESPİTİ

ELİF GÜNDÜZ

İnönü Üniversitesi
Fen Bilimleri Enstitüsü
Moleküler Biyoloji ve Genetik Anabilim Dalı

43+IX sayfa

2024

Danışman: Dr. Öğr. Üyesi Dilek ÇAM DERİN

SARS-CoV-2'nin küresel yayılımı, hızlı tanı sistemlerinin önemini vurgulamış ve güvenilir testlerin geliştirilmesini bir öncelik haline getirmiştir. SARS-CoV-2'nin yapısı ve enfeksiyözlüğünde önemli roller oynayan N ve S proteinleri, güçlü antijenik özellikleri nedeniyle birincil tanı belirteçleri olarak tanımlanmıştır. LFA'lar gibi mevcut tanı yöntemleri, bu viral proteinleri yakalamak için genellikle tek aptamerler veya antikorlar, antikor-aptamer ve antikor-antikor sandviç kombinasyonlarını kullanmıştır. Aptamer kokteylleri ile LFA'nın geliştirilmesi henüz bildirilmemiştir. Bu çalışmada, SARS-CoV-2'nin hızlı ve doğru tespiti için bir mLFA geliştirilmiştir. Çalışmamızda, AuNP'lere konjuge edilmiş aptamer kokteylleri, SARS-CoV-2'nin N ve S proteinlerini ayrı ayrı hedeflemek için kullanılmıştır. Böylece, her iki hedef protein de tek bir test şeridinde aynı anda tespit edilmiştir. Test formatındaki hedeflere bağlanan AuNP-konjuge aptamerler tespit ve etiketleme ajanları olarak kullanılmıştır. Hedef proteine özgü dedektör aptamerleri, bir sandviç kompleksi oluşturmak için test çizgileri üzerinde immobilize edilmiştir. Çalışmamız, dedektör aptamerlerinin test şeridinde konumlandırılmasının testin etkinliğinde önemli bir rol oynadığını göstermiştir. Uygun aptamer yerleşimi tespit doğruluğunu artırırken farklı konumlandırma test verimliliğini azaltmıştır. Genel olarak, hazırlanan mLFA viral tanının yanlış pozitif veya yanlış negatif olasılıklarını ortadan kaldırmış ve LFA sisteminin doğru tanı potansiyelini artırmıştır. Böylece, tasarlanan mLFA kullanımı kolay, ucuz ve doğruluğu artırılmış gerçek zamanlı klinik testler için alternatif bir test prototipi oluşturmuştur.

Anahtar Kelimeler: Çoklu Yanal Akış Tahlilleri, Aptamer Kokteylleri, SARS-CoV-2, N proteini, S proteini

ABSTRACT

Master Thesis

MULTIPLE DETECTION OF SARS- CoV-2 IN POINT-OF-CARE TESTS

ELİF GÜNDÜZ

Inonu University
Graduate School of Nature and Applied Sciences
Department of Molecular Biology and Genetics

43+IX page

2024

Thesis Advisor: Asst. Prof. Dr. Dilek ÇAM DERİN

The global spread of SARS-CoV-2 has highlighted the importance of rapid diagnostic systems and made the development of reliable tests a priority. N and S proteins, which play important roles in the structure and infectivity of SARS-CoV-2, have been identified as primary diagnostic markers due to their strong antigenic properties. Existing diagnostic methods such as LFAs have generally used single aptamers or combinations of antibodies, antibody-aptamer, and antibody-antibody sandwiches to capture these viral proteins. The development of LFA with aptamer cocktails has not been reported yet. In this study, a mLFA was developed for the rapid and accurate detection of SARS-CoV-2. In our study, aptamer cocktails conjugated to AuNPs were used to target N and S proteins of SARS-CoV-2 separately. Thus, both target proteins were detected simultaneously in a single test strip. AuNP-conjugated aptamers bound to targets in the test format were used as detection and labeling agents. Target protein-specific detector aptamers were immobilized on the test strips to form a sandwich complex. Our study showed that the positioning of the detector aptamers on the test strip played an important role in the effectiveness of the test. Appropriate aptamer placement increased the detection accuracy, while different positioning decreased the test efficiency. Overall, the prepared mLFA eliminated the possibility of false positive or false negative viral diagnosis and increased the accurate diagnosis potential of the LFA system. Thus, the designed mLFA constituted an alternative test prototype for real-time clinical testing that is easy to use, inexpensive and has increased accuracy.

Keywords: Multiple Lateral Flow Assays, Aptamer Cocktails, SARS-CoV-2, N protein, S protein

Dedicated to my dear family and myself…

1. INTRODUCTION

1.1 Coronaviruses

Coronaviruses (CoV) are large family of viruses that usually cause mild to severe upper respiratory tract infections in humans. CoVs are host cell-derived, enveloped viruses with viral surface proteins embedded in a lipid membrane [1]. The term corona (Latin: wreath, crown) is derived from the spike (S) proteins that give viruses their distinctive halo-like appearance under the electron microscope. The CoV genome is the largest known genome of a ribonucleic acid (RNA) virus. A common feature of all CoVs is that they are all positively polarized single-stranded RNA viruses [2]. The first human coronaviruses (HCoV), named HCoV-229E and HCoV-OC43, were discovered in the 1960s [3]. These HCoVs are thought to be responsible for about a third of "common cold" cases. Highly virulent CoVs of zoonotic origin, such as Middle East Respiratory Syndrome Coronavirus (MERS-CoV) and Severe Acute Respiratory Syndrome Coronavirus (SARS-CoV), emerged in 2002 and 2012 respectively, caused severe respiratory illness in humans [4]. SARS was first detected in China and caused an 11% mortality rate and MERS was first detected in Saudi Arabia and caused a 37% mortality rate [5,6]. In late 2019, Coronavirus disease 2019 (COVID-19) caused by Severe Acute Respiratory Syndrome Coronavirus 2 (SARS-CoV-2) was emerged in Wuhan, China and leaded to pandemia. Unlike SARS and MERS, which caused localized outbreaks, SARS-CoV-2 quickly passed them both in terms of the number of infected people and the geographic scope of the pandemic [7].

1.2 SARS-CoV-2 Structure and Key Proteins

1.2.1 Structure of SARS-CoV-2

SARS-CoV-2 is a single-stranded, positive-sense RNA virus (+ssRNA) with a genomic size of approximately 30 kb. Initial sequencing revealed a genome of 29,903 nucleotides encoding 9,860 amino acids. This sequencing provided important information about the genetic structure of the virus [8]. The SARS-CoV-2 genome contains structural protein genes-3'-UTR, open reading frames 1a/b (ORF1a/b) and 5' untranslated region (5'-UTR). About two-thirds of the viral genome consists of coding regions for non-structural proteins (nsps), mostly located in ORF1a and ORF1b. These regions encode 16 nsps. Structural proteins such as Spike (S), Membrane (M), Envelope (E) and Nucleocapsid (N)

proteins are encoded by the remaining third of the genome (Figure 1.1A). These structural proteins are essential parts of the SARS-CoV-2, while nsps and accessory proteins such as ORF3a, ORF6, ORF7a, ORF7b, ORF8 and ORF10 assist in the replication of SARS-CoV-2 RNA through various processes within the cell (Figure 1.1B) [9].

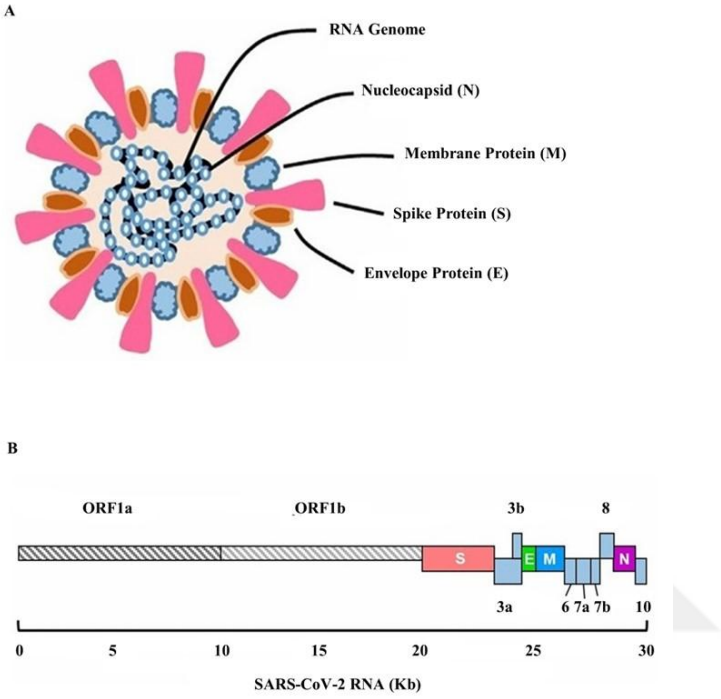

Figure 1.1 Schematic representation of SARS-CoV-2's genome structure. (A) The virus particles and N, M, S, E proteins. (B) Accessory proteins such as ORF1a, ORF1b, ORF3a, ORF3b, ORF6, ORF7a, ORF7b, ORF8 and ORF10 [10].

1.2.2 Role of S protein

S protein of SARS-CoV-2 is a protein that plays a key role in the ability of the virus to enter and infect host cells. Structurally, it is a large transmembrane glycoprotein composed of two functional subunits, S1 and S2. S1 facilitates the initial stages of infection on the viral surface. When the S1 subunit binds to the angiotensin-converting enzyme 2 (ACE2) receptor on the host cell surface via its receptor-binding domain (RBD), the transmembrane protease, serine 2 (TMPRSS2) cleaves the S protein at a specific point, which leads to a conformational change in the protein. This change allows the virus to fuse its envelope with the host cell membrane, allowing the viral RNA to enter the cell and begin replication. This interaction is crucial because binding triggers conformational changes that expose the S2

subunit, which is responsible for membrane fusion [11]. The S2 subunit contains a fusion peptide, heptad repeats (HR1 and HR2), and a transmembrane domain, which plays important roles in fusing the viral membrane with the host cell membrane. The S2 subunit undergoes conformational changes that enable fusion of the viral and host cell membranes and allow viral RNA to enter the host cell [12]. The S protein has become an important target for potential therapies due to the role of the virus in infecting host cells. One of the most effective treatment strategies is to block SARS-CoV-2 binding to the ACE2 receptor on host cells using neutralizing antibodies that prevent the S protein from binding to the RBD. This is a key focus of many COVID-19 vaccines that aim to elicit an immune response [13]. Additionally, early and accurate diagnosis is critical to manage the spread of the virus and initiate timely treatment.

1.2.3 Role of N protein

N protein plays a multifunctional role in the pathogenesis of the virus and interact with viral RNA to form a viral nucleocapsid in a bead-on-strand conformation. It is responsible for encapsulating the viral RNA genome and forms a ribonucleoprotein complex for the protection and packaging of viral RNA within the virion [14]. It consists of an N-terminal domain (NTD) and a C-terminal domain (CTD), with a flexible linker region structurally rich in serine and arginine and they are responsible for RNA binding. This multifunctional protein interacts with the RNA-dependent RNA polymerase (RdRp) complex and other nonstructural proteins, thereby increasing the functionality of the viral genome by facilitating its replication and transcription. It also regulates the host cell to accelerate replication by interfering with antiviral immune responses, such as the interferon signaling pathway, allowing the virus to escape the host immune system [15]. The high conservation of N protein among coronaviruses due to its important role in viral replication, RNA binding and assembly makes it a reliable marker for detecting infection by preserving its basic structural and functional properties. During the SARS-CoV outbreak in 2003, scientists reported that SARS-CoV N protein is a good diagnostic biomarker [16]. Because N protein is stabile in viral variants and species, it has strong immunogenicity, which elicits an immune response in infected individuals and leads to detectable antibody production. Finally, it can be detected in blood samples of SARS patients as early as day 1 after disease onset.

1.3 Diagnostic Methods for SARS-CoV-2

The development of diagnostic methods has become essential for the accurate and rapid detection of COVID-19. Although SARS-CoV-2 has caused fever, cough, gastrointestinal and neurological syndromes in humans [7] it has spread asymptomatically in some patients. For this purpose, molecular testing, Enzyme-linked immunosorbent assays (ELISA), chemiluminescent immunoassays (CLIA), loop-mediated isothermal amplification (LAMP), antigen and serological testing were developed as diagnostic techniques [17] while the reverse transcription polymerase chain reaction (RT-PCR) is the basis of molecular diagnosis of SARS-CoV-2 as it has high sensitivity and specificity for detecting viral RNA [18]. Besides, recent advances in diagnostic methods for SARS-CoV-2 have brought several innovative approaches beyond traditional RT-PCR and antigen testing. One of them is CRISPR technique having a high specificity [19]. Another method, Next-generation sequencing (NGS) that ability to detect not only SARS-CoV-2 but also its variants [20]. Another approach is sensor-based methods for detecting SARS-CoV-2, particularly using optical sensors, immunosensors, and bio-electrochemical sensors [21]. Finally, breath analysis technologies are being explored using sensors to detect volatile organic compounds associated with viral infections, offering a rapid and non-invasive diagnostic method [22].

While recent advances in diagnostic methods for SARS-CoV-2 offer promising solutions, they have also significant limitations. For instance, RT-PCR needs to well-educated personnel because of collecting the swab samples and obtaining the cDNA as a template for amplification and test needs the specific primers and probes that are expensive. Besides, the results can vary from a few hours to several days depending on the collecting of the samples [23]. Although isothermal amplification methods such as LAMP and CRISPR-based diagnostics offer alternatives to traditional PCR by eliminating the need for thermal cycling, they have significant limitations. LAMP is prone to nonspecific amplification that can lead to false-negative and false-positive results if it is not carefully optimized. CRISPR-based diagnostics require a stable and well-protected CRISPR enzyme, which can limit its shelf life and practicality in certain environments [19,24].

Antibodies (IgM, IgG, and IgA) produced by the immune system in response to SARS-CoV-2 infection are detected by serological tests such as ELISA and CLIA, which provide vital information about previous exposure and immunological responses [25,26]. Although they are sensitive and specific they indicate an immune response to past SARS-

CoV-2 infection and can not detect the active infections as antibodies take time to develop [27]. Furthermore, individual differences in antibody production in mild or asymptomatic cases may lead to false-negative results [28].

Sensors used for SARS-CoV-2 detection, including optical and bio-electrochemical types, offer rapid testing advantages but also have limitations. One study developed optical sensors that use gold nanoparticles (AuNPs) to detect viral RNA through refractive index changes, enabling rapid detection [29]. However, specificity issues of this method require precise sensor surface optimization. Bio-electrochemical sensors detect biological elements such as enzymes, antibodies, or aptamers through a chemical reaction that is converted into a measurable electrical signal by an electrochemical transducer. Researches have developed an electrochemical sensor using aptamers to detect SARS-CoV-2 proteins by observing impedance changes as viral particles bind to aptamers [30]. But they faced challenges in stability and long-term use due to the degradation of these elements. At the same time, magnetic sensors [31] and immunosensors [32] have also been used to create diagnostic tools for SARS-CoV-2 detection.

Lateral flow assays (LFAs) were developed as an alternative to these methods. They are inexpensive and do not require specialized laboratory equipment or highly trained personnel which increases their versatility. This makes them suitable for use in a variety of settings including clinics, businesses, schools and even at home. Results can often be obtained within minutes, enabling rapid decision-making in clinical and public health contexts [33]. Overall schematic representation of SARS-CoV-2 diagnostic methods mentioned above is shown in Figure 1.2.

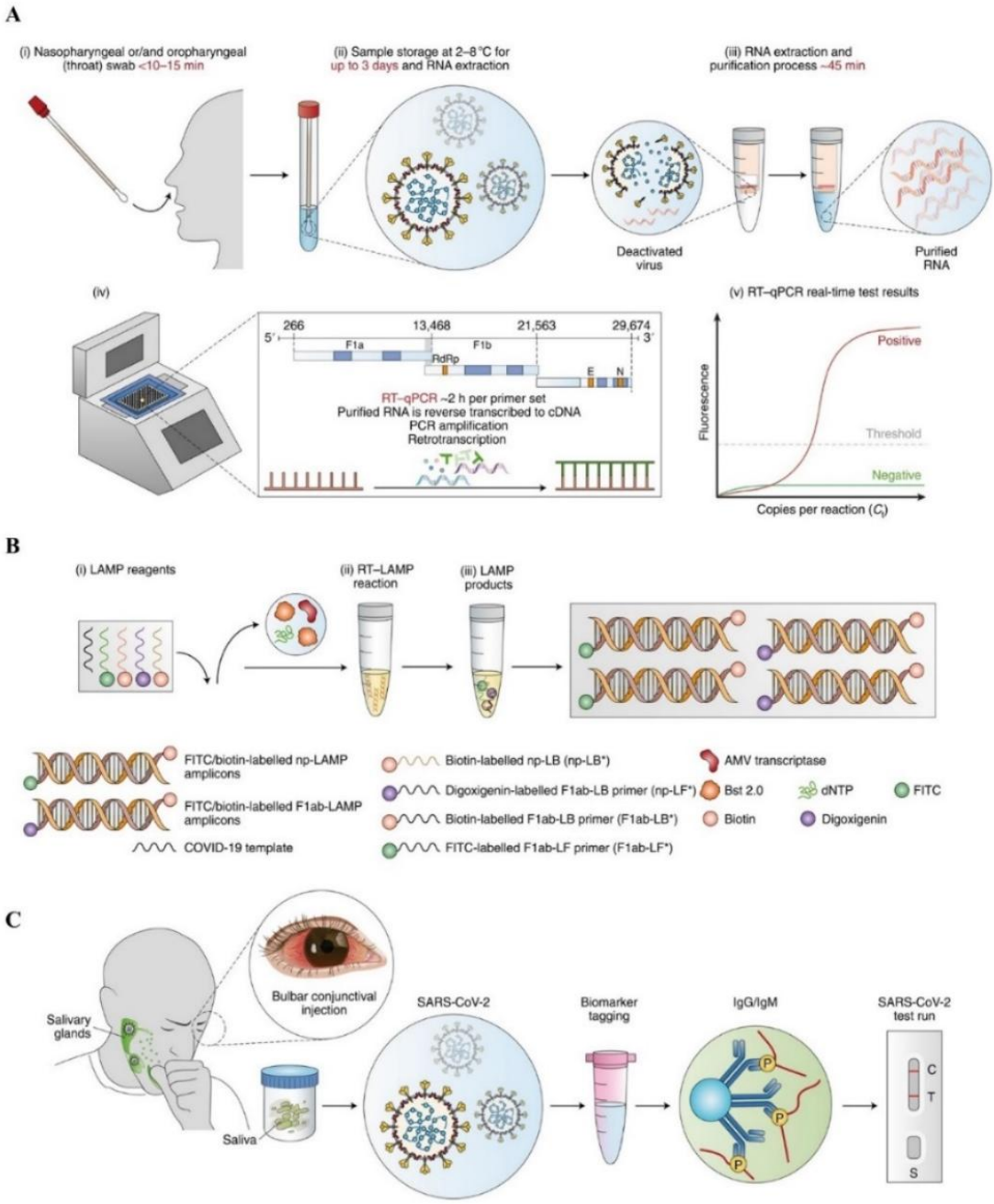

Figure 1.2 Schematic representation of some SARS-CoV-2 diagnostic methods. (A) RT-PCR test. (B) RT-LAMP test. (C) LFA [34].

1.4 Lateral Flow Assays (LFAs)

1.4.1 Principle and mechanism of LFAs

One of the most important point-of-care (POCT) diagnostic tools is LFAs, also called lateral flow immunoassays. LFAs have tremendous potential as an application to improve the rapid detection and control of infections in epidemics or diseases worldwide. They can determine biomarkers in various biological materials and are effective rapid tests for on-site analysis [35]. Pregnancy testing is the first paper-based LFA that can determine the concentration of human chorionic gonadotropin hormone (HCG) in urine samples [36].

Traditional LFAs work on the basis of immunochromatography, a technique that uses capillary action to move a sample along a strip. A sample pad, a conjugate pad, a reaction membrane (usually nitrocellulose membrane), and an absorbent pad are typical components of the strip. Loading the liquid sample (urine, saliva, or blood) containing the target analyte onto the sample pad is the first step of the testing procedure. The target analyte present in the sample is transported along the strip by capillary action. The next component, the conjugate pad, consists of nanoparticles functionalized with an aptamer, an antibody, or an antigen (capture probes). The target analyte in the sample selectively binds to the probes on the nanoparticles as it flows through the strip and forms a complex. These complexes are marked by a visual signal that resembles the red lines and dots formed by AuNPs [35,37]. The complex continues to move along the strip until it reaches a capture region with immobilized probes complementary to the target analyte. When it reaches the test line (TL), it binds to immobilized antibodies or aptamers specific to the analyte, resulting in the formation of a visible line or color change. In LFAs, the test result is based on whether a visible optical signal is present on the TL. The concentration of the target analyte in the sample can also be determined quantitatively using the strength of the signal. As the sample moves toward the control line (CL), the extra probe-conjugate complex interacts with the immobilized molecules unrelated to the target analyte [38] which shows that test is working, correctly. LFAs are also designed to work with small sample volumes usually a few microliters, providing rapid results in 5 to 10 minutes. Thus, rapid response time is critical for applications in areas such as clinical diagnostics, environmental testing, and food safety. The design and principle of LFAs are shown in Figure 1.3.

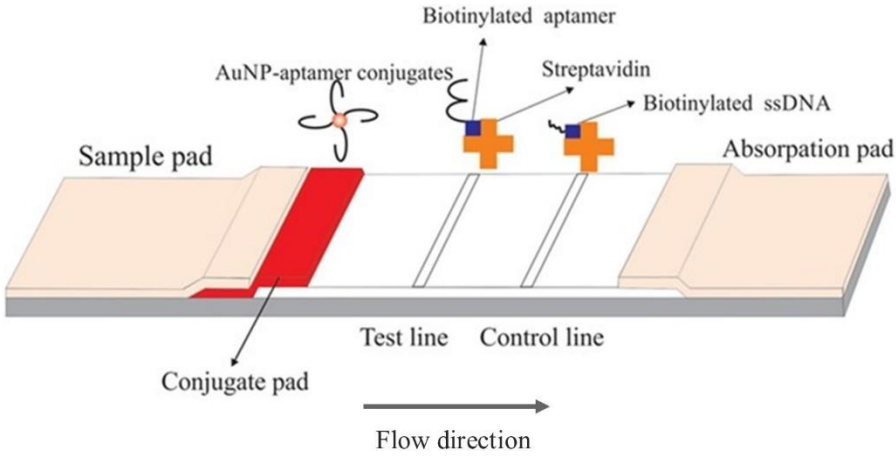

Figure 1.3 A schematic illustration of the design and principle of LFAs [39].

Because of its ease of use, quick results and adaptability to a range of diagnostic settings, LFAs are essential for disease identification. For instance, LFAs have proven to be highly successful in managing disease by identifying viruses including influenza, HIV, and malaria [40]. At the same time, they have been extensively utilized for quick testing during the COVID-19 pandemic, facilitating the infection isolation and identification of the infected people.

1.5 Multiple Detection in LFAs (mLFAs)

Diagnostic technology has advanced significantly with the concept of mLFAs. Multiple line analysis is the simultaneous detection of numerous analytes using multiple test lines on a single strip [41]. mLFAs technique is useful when the multiple related or unrelated analytes needed to be detected simultaneously or when multiple infectious agents are present. Each TL is embedded with distinct capture reagents, such as aptamers or antibodies that bind to various targets. The application of the sample causes it to flow through the strip via capillary action and then interacts with labeled conjugated pad reagents to bind to targets of interest. After moving in the direction of the appropriate TLs, these complexes are captured there and generate lines that can be observed to indicate the presence of targets. Because of its multiplexing capability mLFAs may detect numerous infections, contaminants, or biomolecules at once saving time and resources. They are ideal for POCT diagnostics, food safety testing, environmental monitoring and biological research because

of their speed, accessibility, and ease of use. However, careful optimization is required in the development of mLFAs to ensure the sensitivity and specificity and to avoid cross-reactivity. Once these challenges are overcome, mLFAs can offer comprehensive and effective solutions in various sectors [41].

Multiple detection strategies for SARS-CoV-2 in LFAs provide a range of advantages that improve the diagnostic accuracy. By detecting both the N and S proteins simultaneously, the test's accuracy is greatly enhanced, reducing the likelihood of false negatives and positives [42]. This approach allows for more thorough diagnosis, offering a better understanding of the viral presence and helping to evaluate the infection status. Moreover, the assay's sensitivity may be increased, allowing it to detect lower viral loads, which is essential for early detection and monitoring of asymptomatic individuals. The flexibility of multiple detection also enables the assay to handle different viral variants, as changes in one protein might not impact the detection of the other, ensuring the test's effectiveness even as the virus mutates [43].

Antibody-based LFAs for targeting N and S protein of SARS-CoV-2 have been reported in the literature. For example, one study achieved 97.2% sensitivity and 99.1% specificity for N protein detection of LFAs using monoclonal antibodies [44]. They also developed mLFA that can simultaneously detect both N and S proteins with 96.5% and 95.8% sensitivity, respectively, using a fluorescently labeled double antibody sandwich structure [45]. Although antibody-based LFAs are effective, they have notable limitations. Aptamers have emerged as promising alternatives to antibodies due to their high specificity, ease of production, and stability. Several studies have investigated aptamer-based LFAs for the detection of SARS-CoV-2, but these detections were performed in separate lines [46]. Simultaneous detection of N and S protein in a single line using multiple aptamers as a cocktail in LFAs for SARS-CoV-2 is not available in the literature. In this regard, there is a significant gap in literature.

1.6 Aptamers and Usage in LFAs

Aptamers, which are short, single-stranded DNA or RNA sequences with an average length of 15 to 80 nucleotides, have similar high affinity and specificity as monoclonal antibodies when it comes to binding to certain target molecules. The stability and accessibility of RNA and DNA aptamers, however, are different. Because there is a reactive

hydroxyl group (-OH) at the 2′ position of the ribose sugar, RNA aptamers are less stable chemically. The deoxyribose sugar's 2′ position contains a hydrogen atom (C-H bond) in DNA aptamers, which makes them less reactive and more stable. DNA aptamers are naturally more stable than RNA aptamers due to this chemical difference [47].

Aptamers have the ability to fold into three-dimensional structures, which enables them to attach to a wide range of targets, including whole cells and simple inorganic molecules (Figure 1.4A). Aptamers are also called “chemical antibodies” because of their ability to specifically recognize and bind target molecules [48]. Aptamers offer several advantages over antibodies, making them attractive for a variety of applications. In addition to being non-immunogenic and non-toxic, they are less expensive and easier to produce than antibodies. They are chemically synthesized for consistency and modification and can target a wider range of substances. They are also more stable and resistant to temperature changes. In addition, their smaller size allows for better tissue penetration [49,50]. These characteristics make aptamers perfect for a wide range of uses, including the purification of target molecules from complex mixtures, the development of biosensors, and the performance of medical and therapeutic processes. Nucleic acids, proteins, peptides, small chemical compounds, and even entire cells are among the many targets that aptamers can bind to.

SELEX (Systematic Evolution of Ligands by EXponential enrichment) is a method for creating aptamers, which are short, single-stranded DNA or RNA molecules that can bind to specific target molecules with high affinity. It involves creating a vast library of random sequences, selecting those that bind to the target, amplifying them and repeating the process multiple times to enrich for high-affinity sequences. After sequencing, individual aptamers are synthesized and tested for their binding properties. Further modifications can be made to improve their stability, affinity, and specificity [51,52]. The general scheme of the SELEX method is shown in Figure 1.4.

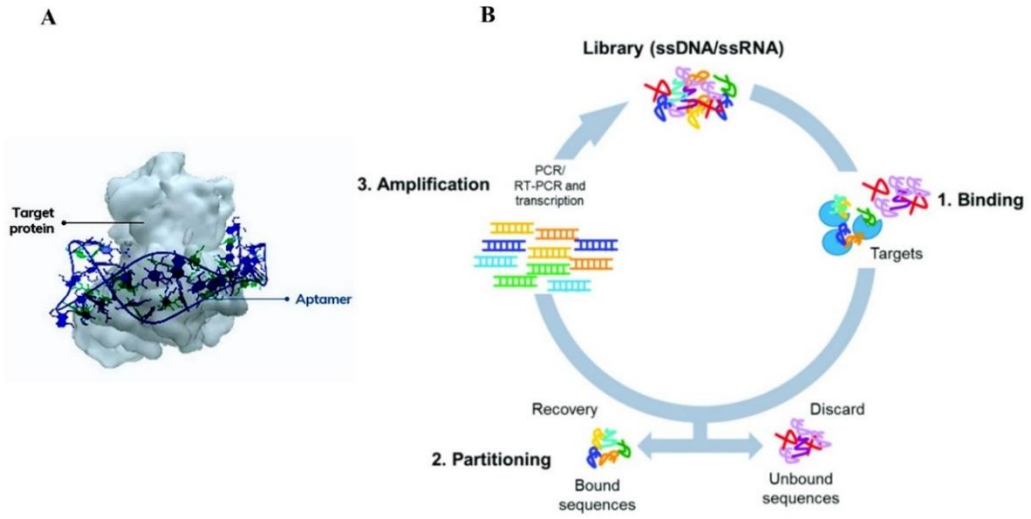

Figure 1.4 The interaction between target-aptamer and general scheme of the SELEX method. (A) Schematic representation the interaction between aptamer and target protein. (B) Summary of SELEX procedure for generation of aptamers for a specific target ligand [53].

During the COVID-19 pandemic, various aptamers were developed to recognize different antigenic regions of SARS-CoV-2, including the N, S, E, and M proteins [54,55]. However, these studies typically relied on single-type aptamer sandwiches or antibody/aptamer sandwiches in the capture zones. In contrast, using an aptamer cocktail, which includes multiple aptamers targeting different epitopes on the same or different proteins, it may offer significant advantages over employing a single aptamer.

1.7 The Role of Aptamer Cocktails in mLFAs

Aptamer cocktails are mainly used to increase the sensitivity and specificity in the detection of target analytes such as proteins or other biomolecules. By combining multiple aptamers that bind to different epitopes on the same target molecule (e.g., different regions of a viral protein such as the SARS-CoV-2 S or N proteins), the cocktails increase the chance of capturing and detecting the target [56]. Using an aptamer cocktail specific for the N and S proteins of SARS-CoV-2 for mLFAs will offer several distinct advantages. First, combining multiple aptamers targeting different epitopes on the same protein increases the sensitivity of the assay by increasing the probability of capturing the target protein even if it undergoes mutations or structural changes. This approach reduces the risk of false negatives

that may arise from changes in the binding site of the target. Second, by incorporating specific aptamers of both the N and S proteins into the assay, simultaneous detection of different viral antigens in the single strip becomes possible, providing a comprehensive diagnostic profile in a single test. This is particularly advantageous in situations requiring rapid and accurate identification of SARS-CoV-2 variants or mixed infections. Third, aptamer cocktails can be optimized to balance the sensitivity and specificity by adapting to the target protein concentrations found in clinical samples. Overall, the use of aptamer cocktails in LFAs to detect the SARS-CoV-2 N and S proteins can increase the stability, versatility and diagnostic reliability of the assay, making it a valuable tool in infectious disease surveillance and management [57].

1.8 Aim of the Study

The aim of this study was to design the rapid diagnostic test for multiple detection of SARS-CoV-2-specific N and S(RBD) regions on the single strip test with mLFA by preparing a cocktail of aptamers with high specificity binding affinity.

2. MATERIALS AND METHODS

2.1 Reagents and Apparatus

All chemicals used in the experiments were of analytical grade. Trisodium citrate and $HAuCl_4.3H_2O$ were provided by Alfa Aesar (Kandel, Germany), while Tris-HCl was obtained from AppliChem (Darmstadt, Germany). KCl and NaCl were sourced from Merck (Darmstadt, Germany). Multicell (Lawrenceville, GA, USA) supplied nuclease-free water and saline-sodium citrate (SSC) buffer. Tris(2-carboxyethyl)phosphine hydrochloride (TCEP) was purchased from Sigma Aldrich (St. Louis, MO, USA). The synthesized gold nanoparticles (AuNPs) and AuNP/capture aptamer conjugates were analyzed using Scanning/Transmission Electron Microscopy (STEM) and an Epoch 2 Plate Reader/Spectrophotometer (BioTek, CA, USA). Ultrapure water was used for all solution preparations. Nitrocellulose membrane cards with different flow rates were obtained from Whatman (GE Healthcare, Dassel, Germany), referred to as membrane 1 (E1) and membrane 2 (E2). The absorbent pad, sample pad, and conjugate pad were purchased from Millipore (Burlington, MA, USA).

Aptamer sequences targeting the N protein (N APT3 and NP) [58] and the sRBD (S APT1, S APT2) [59] were obtained from Integrated DNA Technologies (Coralville, IA, USA) with the required modifications. Thiol-modified aptamers were designated as capture aptamers while biotinylated aptamers served as detection aptamers. The sequences of aptamers and designed sandwich models for aptamer cocktails-based mLFAs were listed in Table 2.1.

Table 2.1 Aptamer sequences and prepared assay models for the aptamer cocktails-based mLFAs.

Multiple Sandwich Models	Aptamer cocktails including capture aptamers	Test Line 1	Test Line 2	Control Line
Model 1	**NP:** 5'-ATC CAG AGT GAC GCA GCA AAC CCA AGC AAA CTA CCT CTA TAC CCT TCG ACC TTC ATC ATG G AAA AAA Thiol – SH	**S APT1:** 5'-Bio- CAG CAC CGA CCT TGT GCT TTG GGA GTG CTG GTC CAA GGG CGT TAA TGG ACA-3'	**N APT3:** 5'-Bio - AAA AAA GCA ATG GTA CGG TAC TTC CGG ATG CGG AAA CTG GCT AAT TGG TGA GGC TGG GGC GGT – 3'	**Complementary to NP:** 5'- TGG GTT TGC TGC GTC ACT CTG GAT AAA –Bio 3'
	S APT1: 5'Thiol- CAG CAC CGA CCT TGT GCT TTG GGA GTG CTG GTC CAA GGG CGT TAA TGG ACA-3'			
Model 2	**NP:** 5'-ATC CAG AGT GAC GCA GCA AAC CCA AGC AAA CTA CCT CTA TAC CCT TCG ACC TTC ATC ATG G AAA AAA Thiol – SH	**S APT2:** 5' Bio ATC CAG AGT GAC GCA GCA TTT CAT CGG GTC CAA AAG GGG CTG CTC GGG ATT GCG GAT ATG GAC ACG T 3'	**N APT3:** 5'-Bio - AAA AAA GCA ATG GTA CGG TAC TTC CGG ATG CGG AAA CTG GCT AAT TGG TGA GGC TGG GGC GGT – 3'	**Complementary to NP:** 5'- TGG GTT TGC TGC GTC ACT CTG GAT AAA –Bio 3'

Table 2.1 (continue) Aptamer sequences and prepared assay models for the aptamer cocktails-based mLFAs.

	S APT2: 5' Thiol- SH-: ATC CAG AGT GAC GCA GCA TTT CAT CGG GTC CAA AAG GGG CTG CTC GGG ATT GCG GAT ATG GAC ACG T – 3'			
Model 3	**NP:** 5'-ATC CAG AGT GAC GCA GCA AAC CCA AGC AAA CTA CCT CTA TAC CCT TCG ACC TTC ATC ATG G AAA AAA Thiol – SH **S APT2:** 5' Thiol- SH-: ATC CAG AGT GAC GCA GCA TTT CAT CGG GTC CAA AAG GGG CTG CTC GGG ATT GCG GAT ATG GAC ACG T- 3'	**N APT3:** 5'- Bio - AAA AAA GCA ATG GTA CGG TAC TTC CGG ATG CGG AAA CTG GCT AAT TGG TGA GGC TGG GGC GGT – 3'	**S APT2:** 5' Bio ATC CAG AGT GAC GCA GCA TTT CAT CGG GTC CAA AAG GGG CTG CTC GGG ATT GCG GAT ATG GAC ACG T 3'	**Complementary to S APT2:** 5' Bio- TTT A CGT GTC CAT ATC CGC AAT CCC GA – 3'

2.2 Synthesis of AuNPs

AuNPs were synthesized by the citrate reduction method of $HAuCl_4.3H_2O$. Briefly, 100 mL of 1 mM $HAuCl_4.3H_2O$ solution in erlenmeyer was boiled with continuous stirring on a magnetic stirrer and then 1% sodium citrate was added. After the color of the solution turned from black to red in approximately 2-3 min, it was left to cool at room temperature. The maximum absorbance value (λ_{max}) of the surface plasmons of AuNPs was measured with UV-Vis spectrum. To prepare the concentrated AuNPs colloidal solution was centrifuged for 30 min and stored at 4˚C to be used for conjugation with capture aptamers.

2.3 Preparation of AuNP labeled N – S Aptamers

For the conjugation, thiol-modified capture aptamers—S APT1, S APT2, and NP—were individually activated with TCEP and incubated for 1 hour. Two different concentrations were used: 4 μM for NP and 8 μM for S APT1 and S APT2. After the activation each reaction was mixed separately with 1 mL of AuNPs and allowed to incubate at room temperature. Following this, 0.01 M phosphate-buffered saline (PBS) was added to the solutions for aging with saline and they were incubated further. The AuNPs were then centrifuged and the resulting pellet was washed twice with a suspension buffer containing phosphate buffer, 0.25% Tween 20, sucrose, and BSA. Finally, the suspension was stored at 4°C in the same buffer.

2.4 Preparation of Aptamer Cocktails and Designing of mLFAs Models

The test strips consist of four main components, sample pad, conjugate pad, nitrocellulose membrane and absorbent pad. Each component was individually prepared and then mixed together [60]. Before the application, the sample pad was treated with Tris buffer solution, then dried at 37°C. The absorbent pad was used without any additional treatment. To prepare the N and S aptamer cocktail, AuNP/capture aptamer conjugates were mixed in an eppendorf tube, then loaded onto the conjugate pad and dried. Biotinylated aptamers and complementary (comp) sequences to the capture aptamers for the test and control lines were immobilized, respectively, by utilizing the streptavidin-biotin interaction. Briefly, 1 mg/mL streptavidin and detection aptamers were mixed and incubated for 1 h. Then, it was centrifuged at 14000 rpm for 15 min using ultracentrifuge tubes and washed twice with PBS. Then, it was processed into nitrocellulose membrane as a test and control line by pipetting.

Virus collection buffer (VNAT), SSC and RB (PBS, 0.1% Tween-20 and 2% BSA solution) were used separately for the sample flow.

Three assay designs were developed as models for mLFAs. The detection order of aptamers in the first (TL1) and second test line (TL2) was varied according to the functional potential of the assay. Model 1 was prepared as S APT1-N APT3-comp to NP, Model 2 was S APT2-N APT3-comp to NP, and Model 3 was N APT3-S APT2-comp to S APT2, which shows the order of lines as TL1-TL2-CL, respectively. Figure 2.1 shows the schematic representation of the working principle of aptamer cocktails-based mLFAs models.

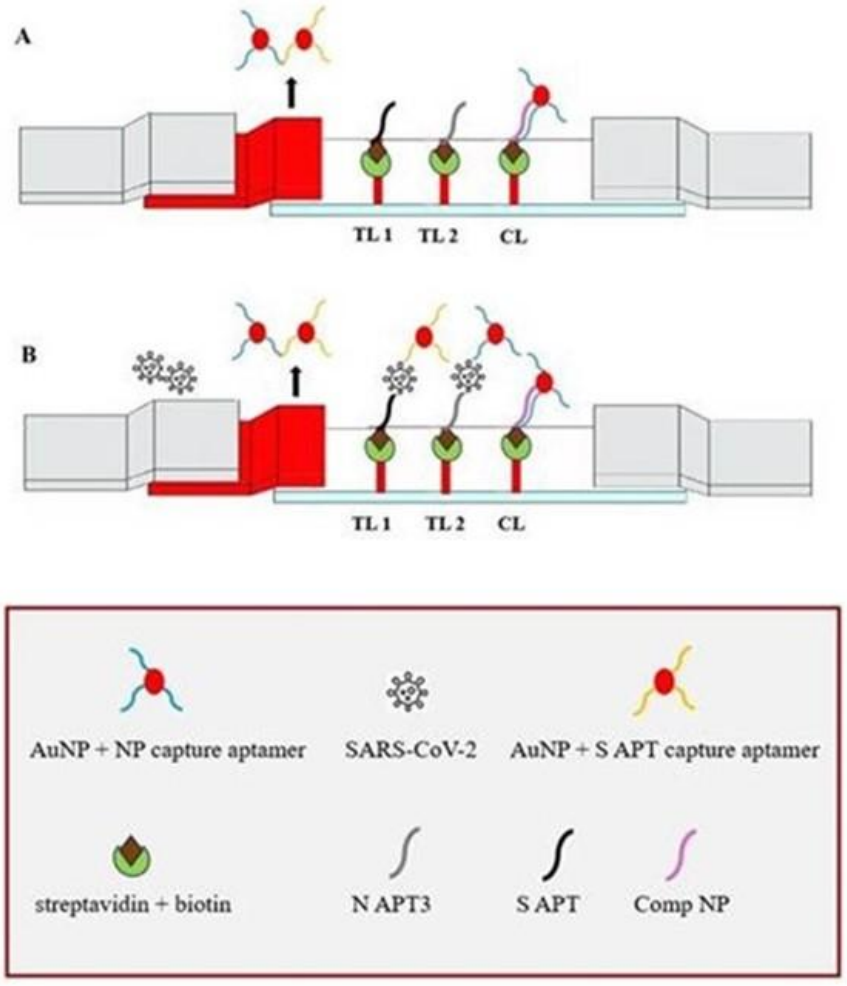

Figure 2.1 Working principle of aptamer cocktails-based mLFAs without (A) and with the target (B).

2.5 Quantitative Color Intensity Analysis

The color intensity after the performance of Model 1 and Model 2 was captured using ImageJ software 1.x (National Institutes of Health (NIH), Bethesda, MD, USA). The color intensity of strong and weak binding in selected strips was compared with the histogram data. Any area on the membrane was selected as the control level of intensity and the presence of weak lines was quantitatively verified based on the control level. A histogram plot was obtained to depict the color intensity on a scale from 0 to 255.

2.6 Clinical Sample Preparation for SARS-CoV-2 Detection

SARS-CoV-2 detection in clinical samples was tested by applying 100 µL of nasopharyngeal or oropharyngeal swab samples, collected in virus collection buffer, onto the sample pad. These swab samples were provided by the Department of Medical Microbiology at Inonu University, Malatya, Türkiye. Prior to use, a random selection of positive and negative clinical samples, confirmed by rRT-PCR, were chosen without regarding to the patients' age, sex, or clinical history, and applied to the mLFAs. The study followed the Declaration of Helsinki guidelines and received approval from Inonu University's Clinical Research Ethics Committee (2023/74). Informed consent was obtained from all participants involved in the study.

2.7 Experimental Strategy

This study involves multiple key steps to enable efficient and accurate detection of SARS-CoV-2 viral proteins by mLFAs. In the first step, AuNPs used as signal-generating labels for analysis are synthesized. These AuNPs are then conjugated with aptamers specific for N and S proteins of SARS-CoV-2, creating labeled probes that can selectively bind to target proteins. In the next step, an aptamer cocktail is prepared that enhances the ability to simultaneously detect both N and S proteins in a single test strip. It then involves designing and assembling mLFA models by optimizing aptamers in the test and control lines of the strip. The analysis workflow involves sample collection and application to the test strip, where the labeled AuNP-aptamer complexes interact with target proteins in the sample. Successful binding results in visible lines indicating the presence of SARS-CoV-2 at specific locations in the strip. This strategy aims to develop a rapid, easy-to-use assay to detect SARS-CoV-2, which is crucial for timely diagnosis and effective monitoring. The general scheme of the experimental strategy is given in Figure 2.2.

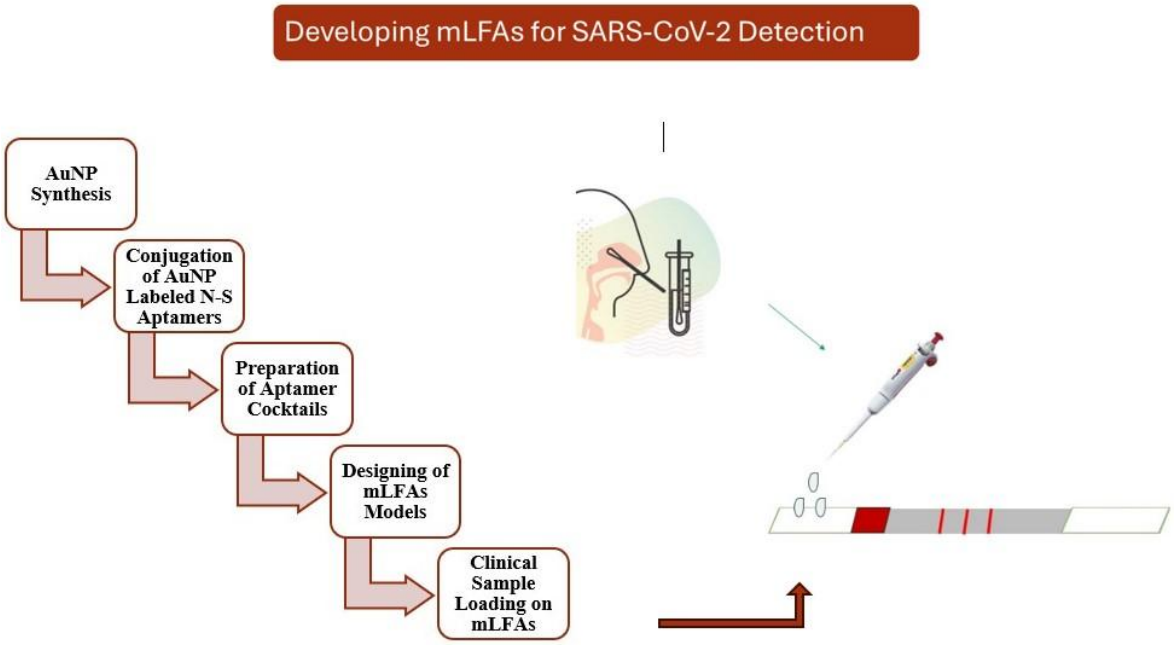

Figure 2.2 Overall of the experimental strategies and methods for SARS-CoV-2 detection in mLFAs.

3. RESULTS AND DISCUSSION

3.1 Synthesis and Characterization of the AuNPs

The homogeneous nature of AuNPs is vital for ensuring stability, enabling surface modifications, and enhancing the reproducibility of assay development, which makes them ideal for use in LFAs. The maximum absorption spectrum (λ_{max}) of the synthesized AuNPs was observed at 521 nm (Figure 3.1A). Colloidal AuNPs showed a uniform size distribution with an average diameter of 13 nm (Figure 3.1B). This also indicates the pure, non-precipitated, and stable state of colloidal AuNPs. As expected, after binding the capture aptamers to bare AuNPs, the λ_{max} shifted to 526–527 nm (Figure 3.1 C-E), reflecting the modification of nanoparticles due to the aptamer coating. The increase in the λ_{max} values in all three conjugates indicates that the capture aptamers were successfully bound to AuNPs. The concentration of capture aptamers on the surface of AuNPs significantly affects the stability and binding on the AuNP surface. 4 μM was chosen for NP and 8 μM for S APT1 and S APT2 and since the stability was achieved at these concentrations and no precipitation was observed the experimental procedure was continued at these concentrations.

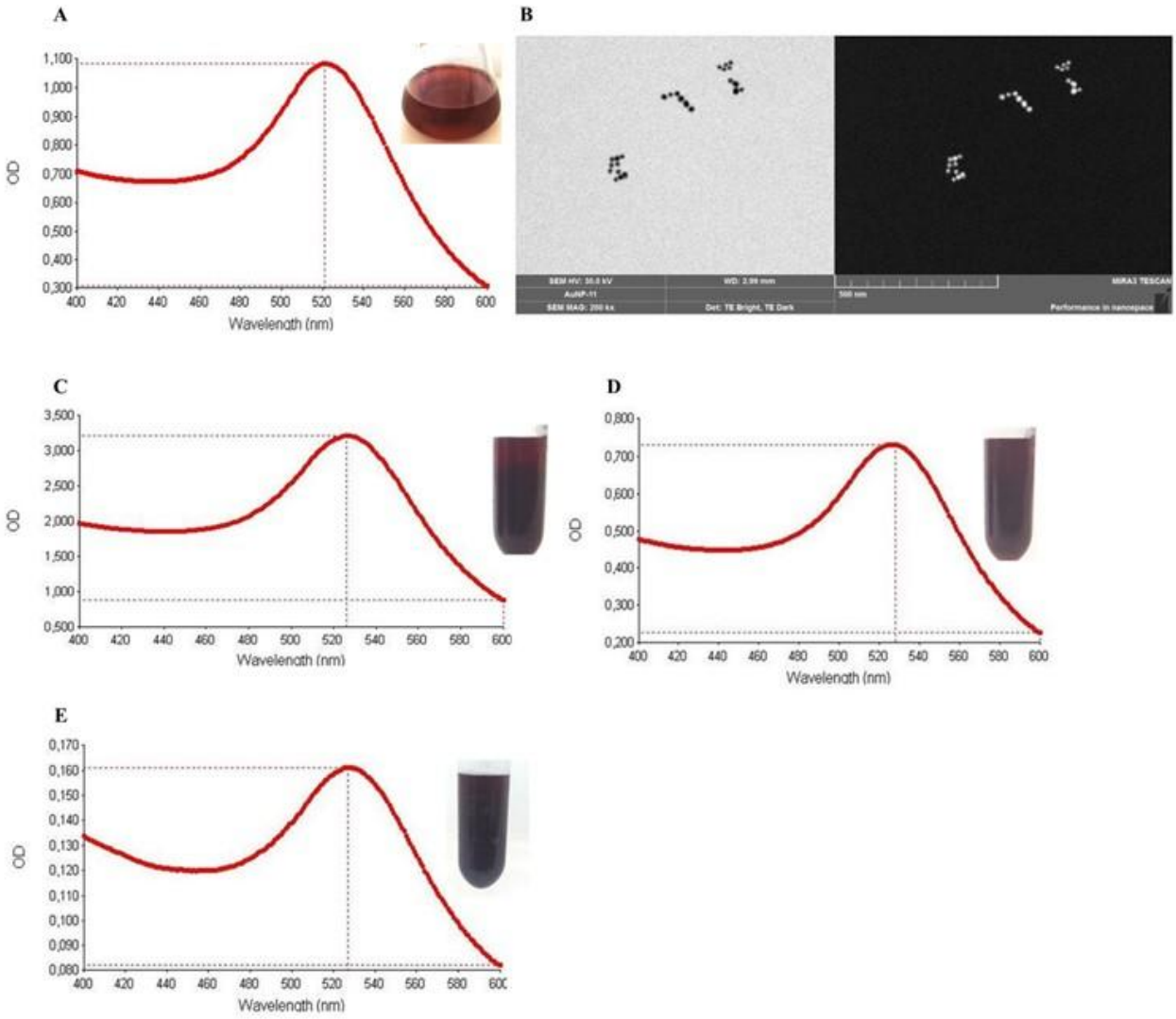

Figure 3.1 UV-Vis spectroscopy (A,B) and size measurement of the synthesized AuNPs by STEM (B). (A,B) Represent the optical properties of naked AuNPs. Shown 8 µM conjugation of S APT1 (C) and S APT2 (D) with AuNPs. (E) Represents the conjugation of 4 µM NP with AuNPs.

3.2 Effect of the Concentrations of Aptamer Cocktails in mLFAs

In order to increase the probability of detection, aptamer cocktail was prepared that simultaneously targets different antigenic regions of SARS-CoV-2, namely N and S proteins, to see its effect on the specificity of the assay. Experiments were performed with two concentrations, 4 µM for NP and 8 µM for S APT1 and S APT2. These concentrations were chosen based on preliminary binding assays (Figure 3.2) in which NP showed a greater

binding affinity than the S aptamer. Interestingly, it was observed that NP used at a 4 μM concentration much lower than the concentration of S aptamer produced a much stronger binding signal than S used at 8 μM, except for line 2 (Figure 3.2) and accordingly a more intense color was formed on TL. These results revealed that NP showed more selectivity towards its target antigen and produced a stronger signal than S even at low concentration. The results also highlighted the importance of carefully selecting and optimizing aptamer concentrations when used as cocktails in LFAs, and mLFAs could be optimized for lower reagent usage while maintaining high sensitivity, making the assays more adaptable for large-scale applications.

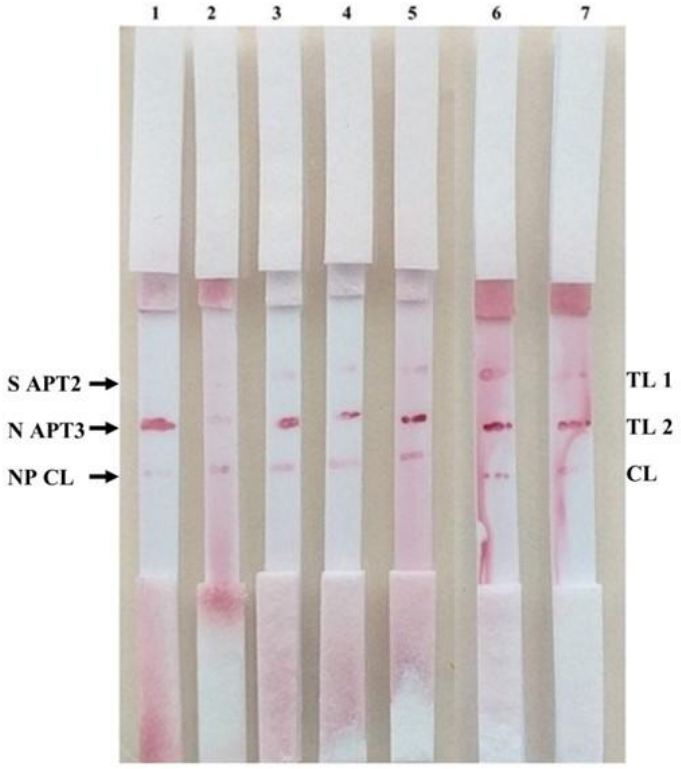

Figure 3.2 Binding affinities of the NP and S aptamers to the SARS-CoV-2 on developed mLFAs. Strips 1-7 were loaded with positive clinical samples. TL1: S APT2, TL2: N APT3, CL: Comp to NP.

3.3 Dual-Target Detection of SARS-CoV-2 in Clinical Specimens with mLFAs

The E1 membrane performed better than the E2 membrane especially in terms of flow rate, binding capacity and detection sensitivity (Figure 3.3). Furthermore, the higher binding capacity of E1 enabled the target analytes to be captured more efficiently, resulting in stronger and more reliable signal intensities (Figure 3.3A strip 3,4). This sensitivity was

particularly important for detecting low analyte concentrations and providing accurate and reproducible results. In contrast, the E2 membrane exhibited slower flow rates and lower binding efficiency, compromising the overall sensitivity and consistency of the experiment (Figure 3.3B). Due to these results, E1 was selected as the most suitable membrane for all experimental models to provide the best performance. The experimental performance comparison of the E1 and E2 membranes is shown in Figure 3.3.

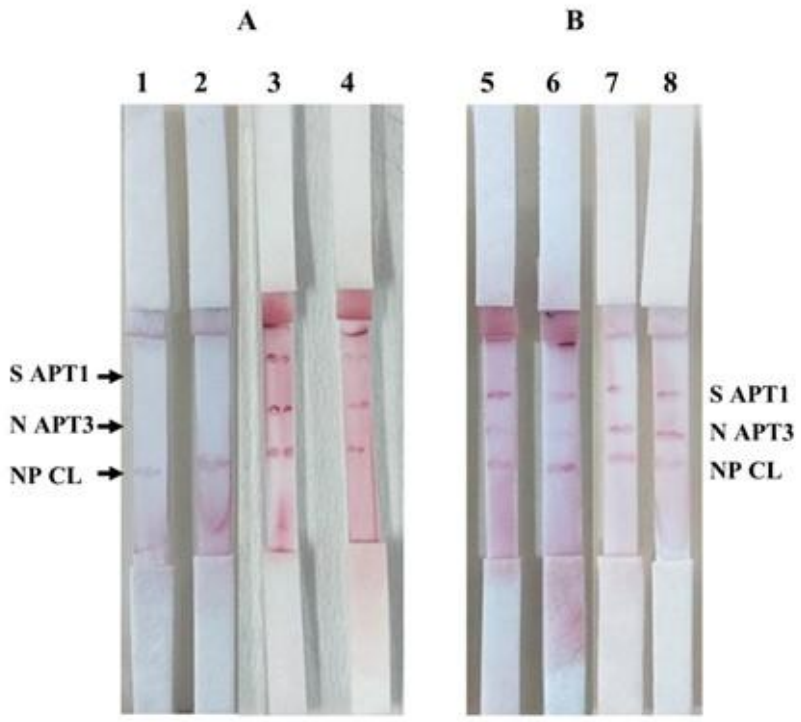

Figure 3.3 Comparison of E1 and E2 membrane in mLFAs developed by Model 1. (A) E1 membrane. Strips 1-2 were loaded with negative clinical samples. Strips 3-4 were loaded with positive clinical samples. (B) E2 membrane. Strips 5-6 were loaded with negative clinical samples. Strips 7-8 were loaded with positive clinical samples. TL1: S APT1, TL2: N APT3 and CL: Comp to NP

To compare the effectiveness of each aptamer, LFA using NP and S aptamers separately was also designed. The results showed that the NP aptamer exhibited a stronger affinity than the S aptamer in detecting both N and S proteins in separated strips (Figure 3.4). The results may also be due to the structural stability and compact conformation of the N protein, which allows stronger and more specific interactions with its corresponding aptamer. In contrast, the S protein, with its dynamic structure and conformational variability, exhibits less stable interactions. This structural difference likely contributes to the reduced sensitivity

in detecting the S protein, which is further complicated by its variability and lower abundance compared to the N protein [61].

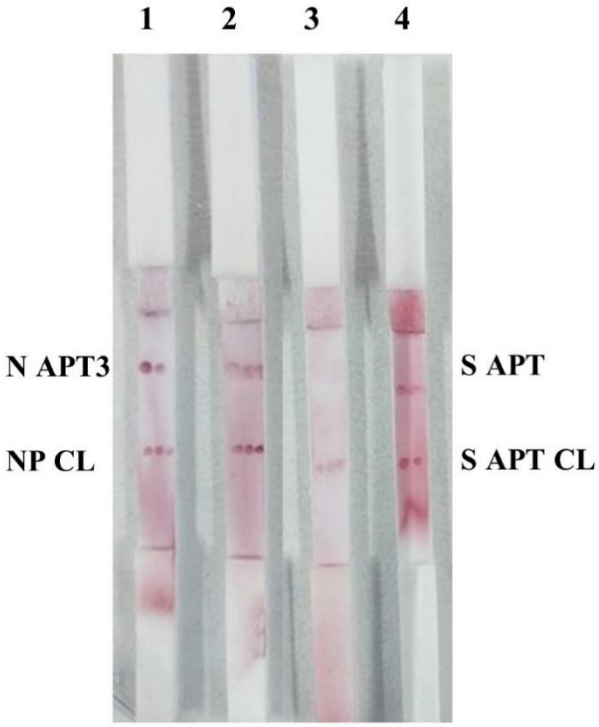

Figure 3.4 Comparison of binding affinities of N and S aptamers on separate strips. Strips 1-2 were loaded with positive clinical samples using the N aptamer. Strips 3-4 were loaded with positive samples using the S aptamer.

3.3.1 Model 1 assay performance

For Model 1, initially, validated clinical samples from the same patient were applied separately as a test number of 10 strips with the negative and positive clinical sample. It was clearly seen that mLFA prepared by Model 1 worked correctly because of having clear CLs for the applied positive and negative swab samples (Figure 3.5). Therefore, this model was used for testing more clinical samples to see the specificity and sensitivity of the assays. For this purpose, positively confirmed 30 and negatively confirmed 30 different naso/oropharyngeal swab samples collected directly from the individuals with suspected COVID-19 were applied to mLFA prepared by Model 1. Compared to single aptamer-based LFAs [62,63], our developed mLFAs provide a complete diagnostic tool that can confirm the presence of the virus via multiple targets. This is particularly important in cases where

the virus may mutate and change the antigenic site targeted by a single-target-specific aptamer. Furthermore, the results confirmed that even if a weak signal was produced in one line on the strip, the other line detected the presence of the virus. As shown in Figure 3.5, the developed mLFA were successfully identified the negative (A) and positive clinical samples (B), with no evidence of nonspecific interference. Although TL1 of lines 1,7,9,11,26,28 was not detected by naked eye (Fig. 3.5B), the presence of the virus was verified using ImageJ software. In order to compare the color intensity, a histogram plot of the strips 7 and 18 shown in Fig. 3.6 was generated. For the strip 18 which showed visible signals to the naked eye, the histograms for TL1 (Figure 3.6A), TL2 (Figure 3.6B), and CL (Figure 3.6C) revealed high average intensities of 173.604, 185.100 and 185.062, respectively. These intensities showed strong and consistent signals with high mode values and broader distributions confirming the presence of high concentrations of target proteins in this strip. This robust signal response demonstrated that the captured and detected the presence of the proteins probably present at higher concentrations. In contrast, strip 7 which did not show the visible lines to the naked eye, had much lower average intensities for TL1 (Figure 3.6E) and TL2 (Figure 3.6F) and was closer to the background level observed in an empty region of the membrane (Figure 3.6D) chosen as the control level. The average intensities for TL1 and TL2 in strip 7 are 182.549 and 183.527, respectively and the narrow distributions indicate weak signals that can be distinguished from the background. Although these weak signals were insufficient for visual detection, the color based analysis revealed the slight peaks (Figure 3.6 E,F) as a quantitative. This sensitivity revealed by the low peaks in the histogram, emphasized that detection can occur quantitatively in mLFAs even if detection is not possible with the naked eye.

Weak binding on some strips may be due to differences in viral load or swab composition among patients, which may affect the ability of the S aptamer to bind to the target. Additionally, using the same aptamer as both the capture and detection in the sandwich format could result in weaker detection, as opposed to a dual-aptamer sandwich format that may provide stronger signal detection [65]. When TL2 was compared with TL1, other strips were quite distinct (Figure 3.5B) except for stripes 26-27. The strong detection is attributed to the high affinity and effective binding properties of the N aptamers especially when utilized in aptamer cocktails, which capturing the N protein and making them ideal for the assay. In contrast, while the S aptamers also recognized their target, the N aptamers

provided more reliable and consistent results. This suggests that in Model 1, N aptamers offer greater potential for multiple assays.

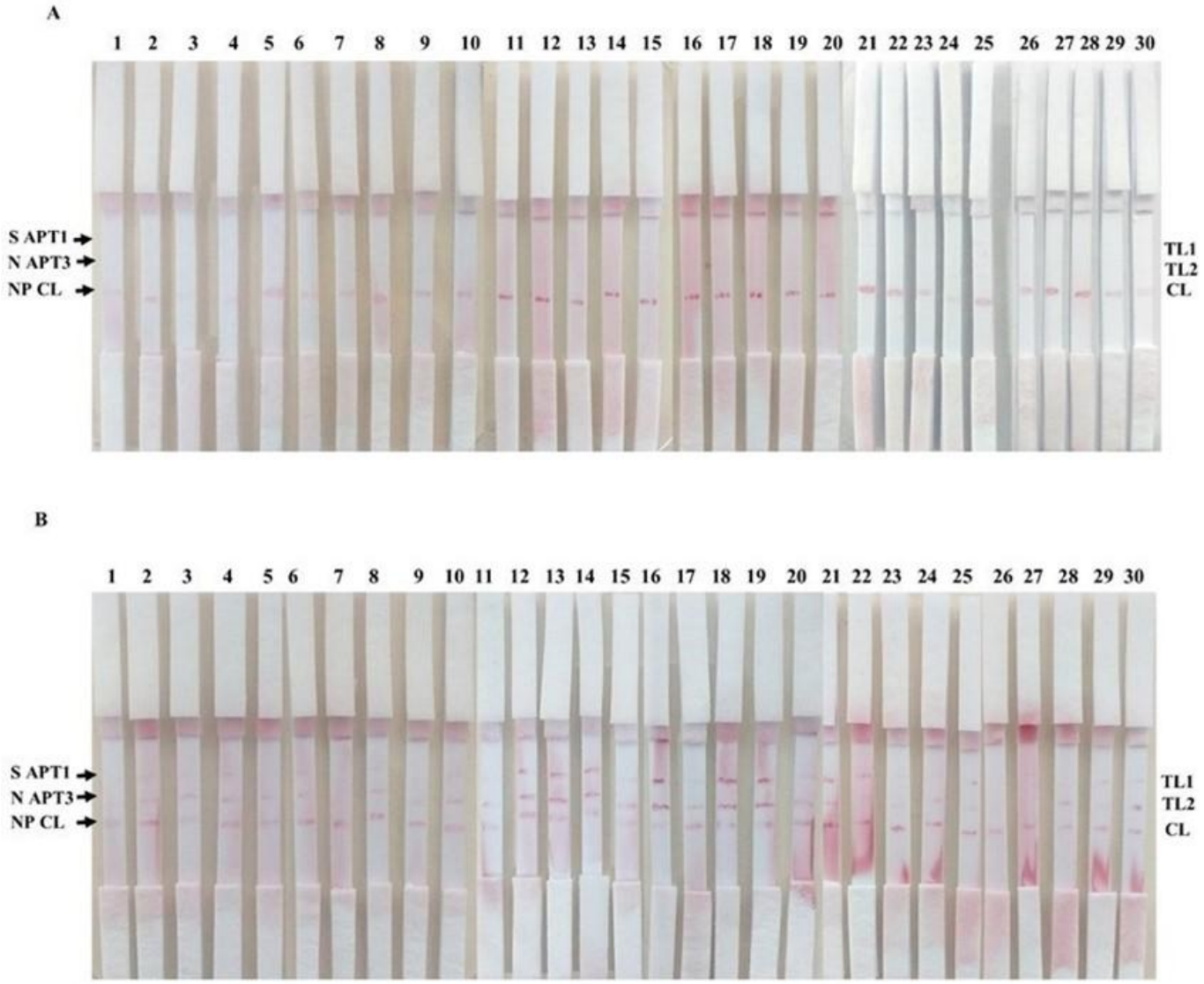

Figure 3.5 SARS-CoV-2 detection in naso/oropharyngeal swabs on mLFAs developed by Model 1. Negatively (A) and positively (B) confirmed swabs samples from different patients. TL1: S APT1, TL2: N APT3 and CL: Comp to NP

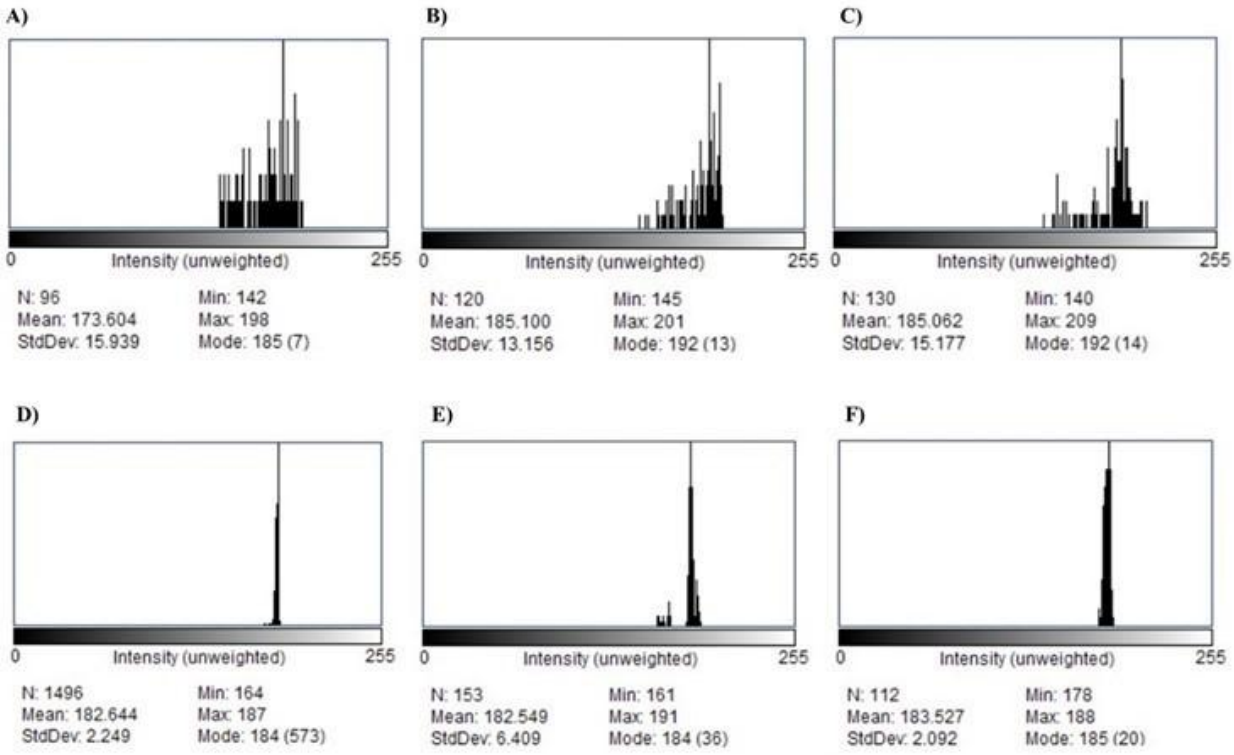

Figure 3.6 Histogram graph generated by using ImageJ software for Model 1. (A) TL1 color intensity of strip 18. (B) TL2 color intensity of strip 18. (C) CL color intensity of strip 18. (D) Control group, strip without virus loading. (E) TL1 color intensity of strip 7. (F) TL2 color intensity of strip 7.

3.3.2 Model 2 assay performance

The mLFAs developed by Model 2 also accurately detected the SARS-CoV-2 in clinical samples, as in Model 1 (Figure 3.7). However, in lines 27-28, the color intensity on TL1, TL2, and CL was noticeably weaker than in other lines, which may be attributed to the lower concentration of viral particles in those clinical samples or variations in the preparation of the test. Except for these strips, both negative (Figure 3.7A) and positive samples (Figure 3.7B) were clearly detected in each strip without any false positive/negative results. The quantitative analysis shown in the histogram graph (Figure 3.8, A-F) showed the presence of lines in strip 26 where intense color was detected and in strip 27 where binding was too weak to be seen. For strip 26 which showed visible signals, the histograms for TL1 (Figure 3.8A), TL2 (Figure 3.8B) and CL (Figure 3.8C) showed high average intensities of 184.200, 182.798 and 178.060, respectively with relatively broad distributions. This suggests a significant abundance of the target protein at this line. Consistent high peaks across TL1,

TL2 and CL indicate that the aptamers bind strongly to N and S proteins, confirming the effectiveness of the assay when virus levels are sufficient. In contrast, strip 27 which showed no visible signal, had low intensity peaks at TL1 (Figure 3.8D), TL2 (Figure 3.8E) and CL (Figure 3.8F) and the average intensities were closer to the background (approximately 198–200). The narrow distribution of these peaks, especially in TL1 and TL2, indicates a weak signal and suggests a low target protein concentration that falls below the visual detection threshold. Overall, the histogram analysis provided both qualitative and quantitative information about the presence of SARS-CoV-2 protein in the test strips. At the same time, multiple lines were prepared to ensure detection even if a target was not visually recognized in a single line. Thus, this showed the importance of using and developing the mLFAs instead of single TL based LFAs which can be resulted with false negative [65]. A key improvement in this model was the significantly stronger color intensities across the lines compared to Model 1. This enhanced signal, particularly on TL1, can be attributed to the use of S APT2, an aptamer with a higher affinity for its target than S APT1, which was used in Model 1. The superior binding efficiency of S APT2 facilitated a more effective interaction with the target, resulting in stronger and more easily detectable signals, thereby enhancing the overall assay performance. This emphasizes the importance of aptamer selection, where the type, affinity, and binding capacity of the aptamers are crucial for optimizing signal amplification and sensitivity in mLFAs. Additionally, the use of S APT2 in the sandwich format did not negatively affect the capture efficiency, which contrasts with the performance of S APT1 in Model 1. This further highlights the critical role of selecting the right aptamer for maintaining efficient capture and detection under different environmental conditions. While there was no significant difference in the detection of the S and N proteins on TL1 and TL2, respectively, the recognition of the N protein was slightly stronger to that of the S protein in the multiple assay (Figure 3.7B). This is likely due to the higher affinity and stronger binding potential of the N aptamers to their target, compared to the S aptamers.

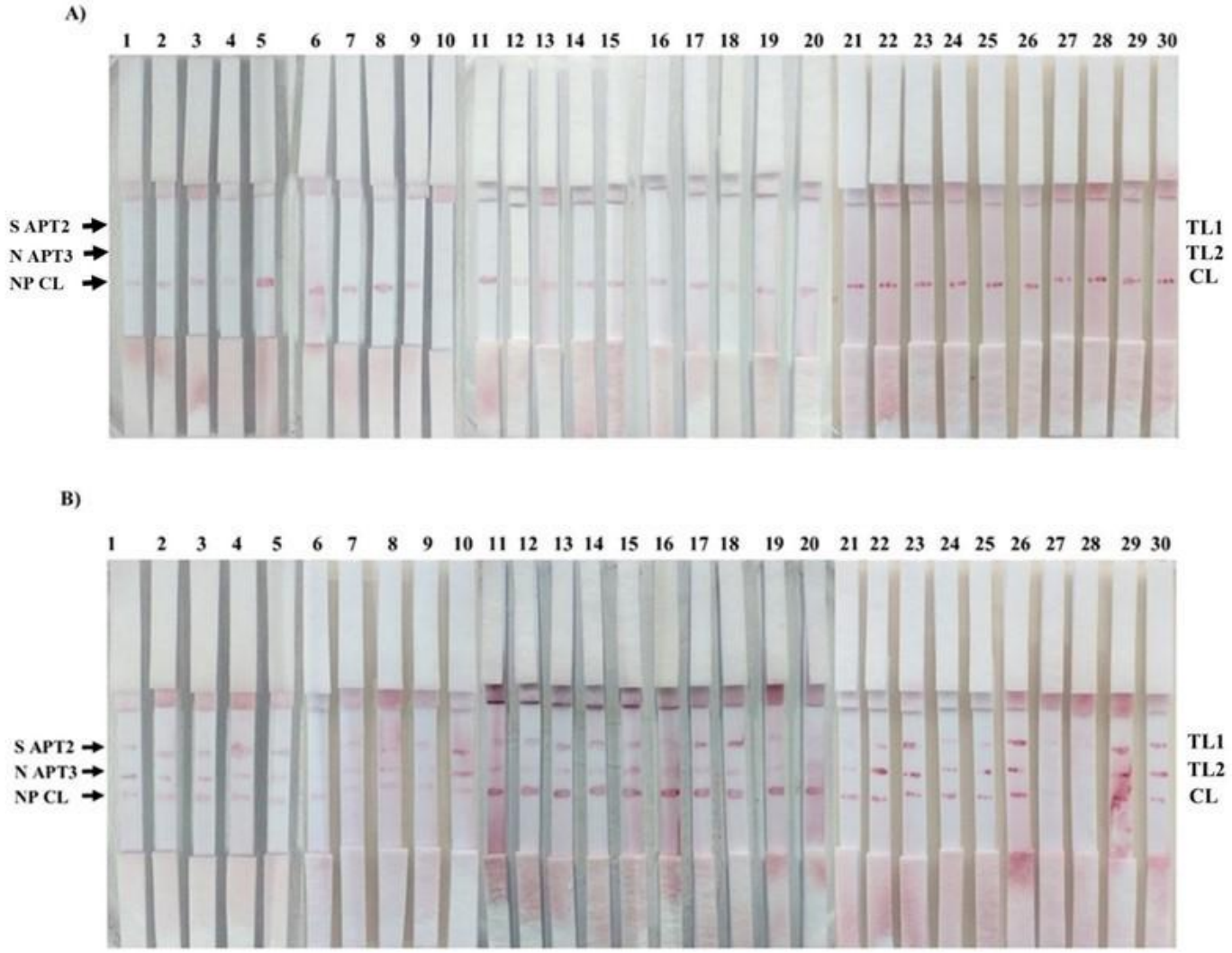

Figure 3.7 SARS-CoV-2 detection in naso/oropharyngeal swabs on mLFAs developed by Model 2. Negatively (A) and positively (B) confirmed swabs samples from different patients. TL1: S APT2, TL2: N APT3 and CL: Comp to NP

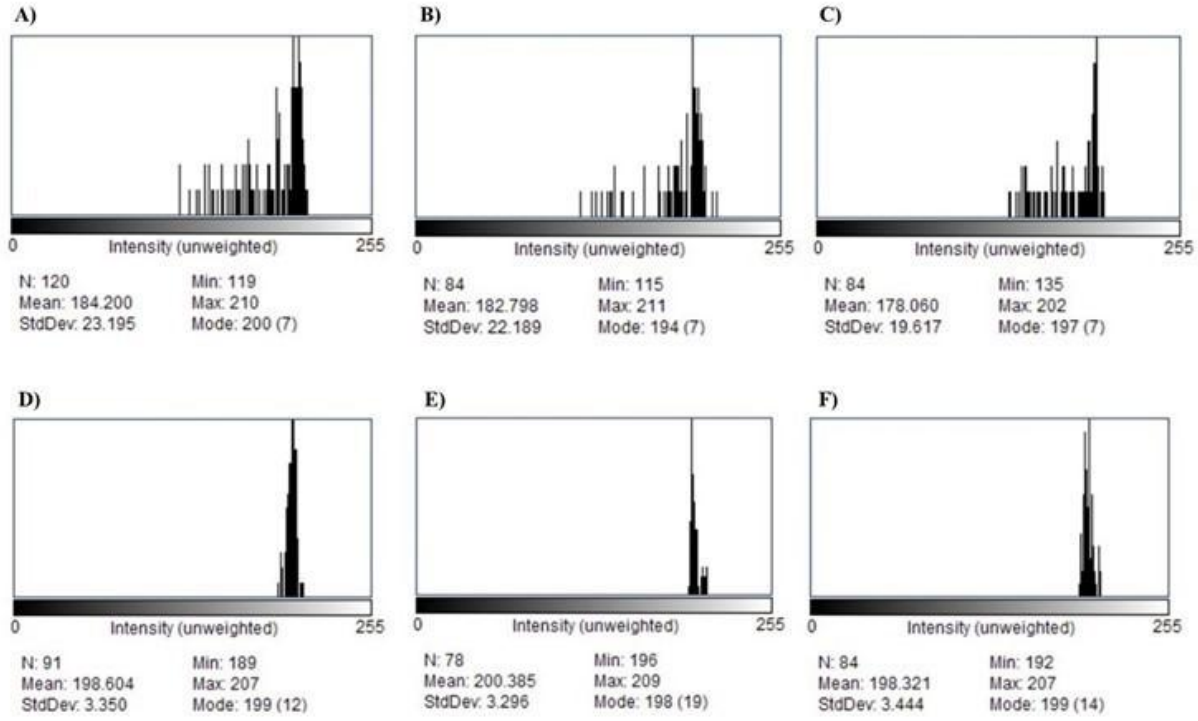

Figure 3.8 Histogram graphs generated by using ImageJ software for Model 2. (A) TL1 color intensity of strip 26. (B) TL2 color intensity of strip 26. (C) CL color intensity of strip 26. (D) TL1 color intensity of strip 27. (E) TL2 color intensity of strip 27. (F) CL color intensity of strip 27.

In Model 1 and Model 2, the capture aptamer is the same as the aptamer immobilized on the TL. In Model 1, S APT1 was conjugated with AuNP and S APT1 was drawn on the TL. In Model 2, S APT2 was conjugated with AuNP and S APT2 was immobilized on the TL. Each aptamer was designed to bind to a specific region or epitope of the S protein, and when the same aptamer was used for both the conjugation and immobilization (on the TL), the binding sites of the aptamer were optimized to recognize the same region of the target, which provided efficient capture and detection. However, as shown in Figure 3.9A, when S APT1 was conjugated on AuNP and S APT2 was immobilized on the TL, the desired test performance could not be achieved due to the fact that these two aptamers could target different regions of the S protein, and nonspecific binding was observed in negative samples. Likewise, the assay did not work properly when S APT2 was conjugated onto AuNP and S APT1 was immobilized in the TL (Figure 3.9B). If two aptamers bind to incompatible epitopes on the S protein, the protein may not be captured correctly, weakening the signal or preventing detection altogether. Furthermore, differences in binding kinetics and affinities

between S APT1 and S APT2 may affect their ability to bind to the same target. This mismatch in binding behavior causes the assay to fail to function properly when different aptamers are used for conjugation and immobilization. In this context, aptamer specificity and binding affinity should be carefully optimized in the design of multiple experiments. In summary, this explains why the assay works only when the same aptamer is used for both conjugation and immobilization but fails when different aptamers are used.

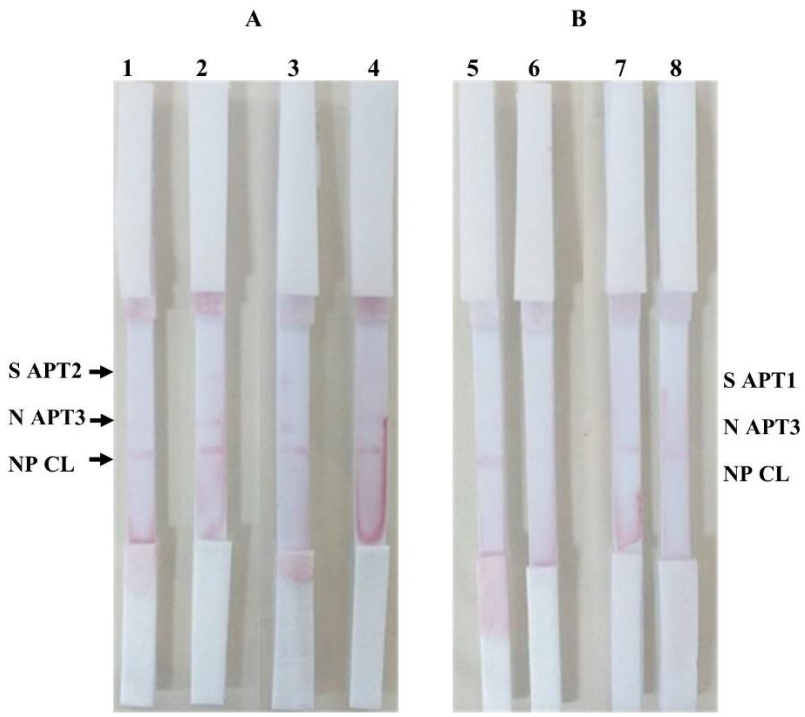

Figure 3.9 Design of the developed mLFAs with different aptamer pairs in conjugation and TL immobilization. (A) S APT1 was used for conjugation and S APT2 for immobilization. Strips 1-2 were loaded with negative clinical samples, and strips 3-4 were loaded with positive clinical samples. (B) S APT2 was used for conjugation and S APT1 for immobilization. Strips 5-6 were loaded with negative clinical samples, and strips 7-8 were loaded with positive clinical samples.

3.3.3 Model 3 assay performance

The desired experimental result could not be obtained in Model 3. When loading was performed with negative clinical samples, nonspecific binding was observed (Figure 3.10A), and binding was much weaker than Model 1 and Model 2 (Figure 3.10B) with the applied positive clinical samples. At the same time, the binding signal of S aptamer in strips loaded with positive clinical samples was almost negligible compared to N aptamer. According to these results, the reason for the failure of Model 3 may be due to the aptamer immobilized

on CL. While complementary to NP was used as CL in Model 1 and Model 2, complementary S APT2 was used as CL in Model 3. As it is seen clearly, it is possible to say that CLs are more intense when the assay was prepared complementary to NP (Models 1 and 2) compared to CLs prepared as complementary to S aptamer conjugates (Model 3). This suggests that the S aptamer may not bind to its target protein as consistently or strongly as the N aptamer. Furthermore, nonspecific binding in negative clinical samples in Model 3 may be due to low abundance or structural variations in the S protein, leading to less effective binding by the S aptamer. Overall, the use of the N protein aptamer as the CL in Models 1 and 2 was a critical factor in the successful performance of these assays and increased both the stability and specificity of the assay. This highlights the importance of targeting highly conserved viral proteins such as N protein for both detection and control line functionality in diagnostic assays as it provides a more reliable platform for consistent results. Furthermore, these results also demonstrated the importance of the position of aptamer duplexes and detection aptamers in mLFAs. Since the capture of N proteins was reduced in Model 3, i.e. N APT3 was placed in TL1, whereas in Model 2, N APT3 was placed in TL2. This result is similar for S protein detection as well. Since the detection was reduced when S aptamer was used in TL2 (Model 3) compared to the position in TL1 (Model 2). Therefore, it has been observed that the position of the detection aptamer is important and affects the test efficiency depending on the aptamer type. Thus, this finding could be useful for mLFAs having a lack of the importance of the aptamer and antibody localization in current diagnostic research.

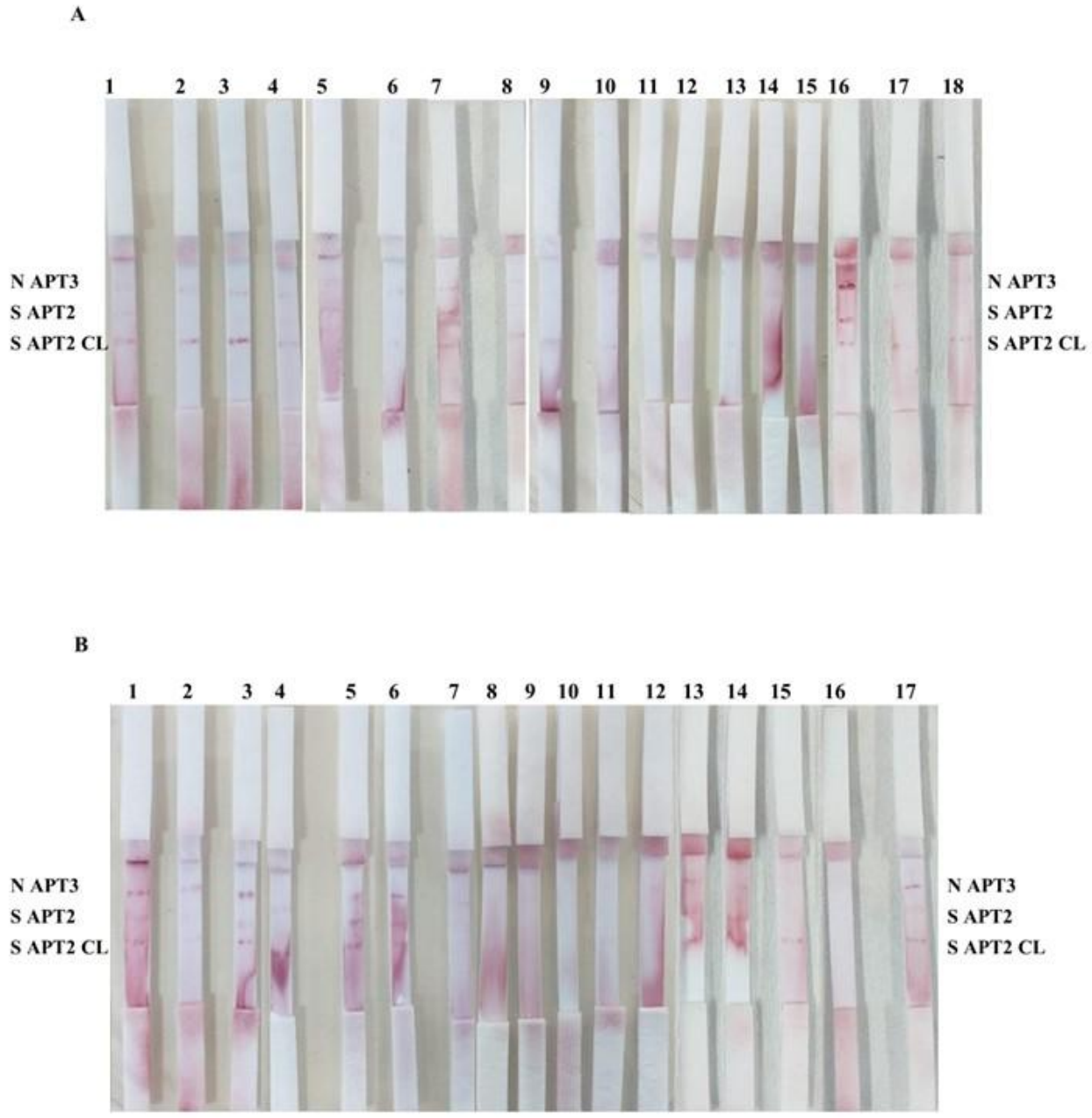

Figure 3.10 SARS-CoV-2 detection in naso/oropharyngeal swabs on mLFAs developed by Model 3. Negatively (A) and positively (B) confirmed swabs samples from different patients. TL1: N APT3, TL2: S APT2 and CL: Comp to S APT2

Although there is a wealth of literature on the development of LFAs utilizing antibodies or aptamers for viral detection, most of the research emphasizes improving the binding affinity, specificity, or chemical modifications of aptamers to enhance the assay sensitivity. These studies commonly focus on either single test strips or the use of multiple

antibodies for detection. However, the specific influence of the order and spatial arrangement of aptamers on the overall assay dynamics has not been thoroughly explored. Our study highlights that the location of aptamers on the test strip can significantly impact whether the test works correctly.

3.3.4 Sensitivity and specificity of mLFAs

The sensitivity and specificity of the developed mLFAs were calculated separately and the effects of different models on these parameters were analyzed [66]. Initially, the specificity and sensitivity of Models 1 and 2 were evaluated according to the visibility of at least one TL among multiple lines present in the strip. Additionally, the sensitivity and specificity of individual test lines for the detection of N and S proteins in the same strip were evaluated. As a result, the specificity of all models was found to be 100%. In terms of the sensitivity, Model 1 showed an overall sensitivity of 96.6%. When examined in more detail, the sensitivity for detecting S protein in the TL1 was 80%, while it was 93% for N protein in the TL2. In contrast, Model 2 exhibited excellent sensitivity, reaching 100% for both overall detection and individual detection of S protein in TL1 and N protein in TL2. This indicated that Model 2 was more reliable for the simultaneous detection of both viral targets. These findings highlight the increased sensitivity of LFAs when designed in a multiplex format, allowing for the simultaneous detection of multiple viral proteins, compared to assays using a single test lane. As demonstrated in Model 2, the ability to detect both N and S proteins in a single lane improved the assay performance, providing a more robust diagnostic tool.

Our study compared the single-target LFAs with mLFAs, highlighting the limitations of single-target LFAs, particularly when the target protein is mutated or expressed at lower levels. In such cases, single-target LFAs may experience reduced sensitivity and specificity, as their performance is closely connected to the presence and integrity of a particular viral protein. In contrast, mLFAs decrease these risks by simultaneously targeting multiple proteins, reducing the impact of viral mutations in protein expression on overall assay performance. This approach allows the detection of other target proteins to maintain the reliability of the assay, even if one protein is altered or less abundant. Additionally, designed mLFAs offer several key advantages compared to traditional antibody-based LFAs. The stability of aptamers is particularly useful in ensuring a longer shelf life and consistent performance of the assay. In addition, the production of aptamers is less costly and more

scalable than the production of antibodies, significantly reducing manufacturing costs. These factors make mLFAs not only cost-effective but also highly suitable for mass production and distribution in settings where laboratory access is limited. These advantages position mLFAs as a practical and innovative tool for widespread viral diagnostics.

4. CONCLUSION

In this study, a cocktail of N and S aptamers was used to develop mLFAs for the rapid and accurate detection of SARS-CoV-2 on the single test strip. Results illustrated the high sensitivity and specificity on the E1 membrane with two different models (Model 1 and Model 2) when a cocktail of 8 μM S protein capture aptamers and 4 μM N protein capture aptamers were used. The strips generated using these models showed consistency in the basic analysis principles, including fluid flow through the membrane and time required for visual analysis. Nonspecific binding was observed only in Model 3 which the CL was prepared by S aptamer. The findings highlighted the importance of the aptamer localization in the capture sites, the effects of aptamer concentration and membrane type on the overall performance of mLFAs. By carefully optimizing these parameters, the designed test strips reliably detected both the positive and negative clinical samples within 5–7 min, making them suitable for visual inspection. Moreover, the cocktail-based approach allowed the simultaneous detection of multiple antigenic targets by binding different aptamers to the different viral structures. This approach increased the accuracy of the test as it increased the probability of capturing relevant antigens during testing. The improved accuracy of the test indicated that mLFAs have potential as a strong candidate for multiplex testing not only for SARS-CoV-2 but also for future outbreaks caused by different viruses. The designed models can be easily adapted to the new rapid tests for emerging viral pathogens, which makes it a valuable tool for early diagnosis in clinical settings.

REFERENCES

[1] **Ludwig, S., & Zarbock, A.** (2020). Coronaviruses and SARS-CoV-2: A Brief Overview. Anesthesia and analgesia, 131(1), 93–96. https://doi.org/10.1213/ANE.0000000000004845

[2] **Naqvi, A. A. T., Fatima, K., Mohammad, T., Fatima, U., Singh, I. K., Singh, A., Atif, S. M., Hariprasad, G., Hasan, G. M., & Hassan, M. I.** (2020). Insights into SARS-CoV-2 genome, structure, evolution, pathogenesis and therapies: Structural genomics approach. Biochimica et biophysica acta. Molecular basis of disease, 1866(10), 165878. https://doi.org/10.1016/j.bbadis.2020.165878

[3] **Liu, D. X., Liang, J. Q., & Fung, T. S.** (2021). Human Coronavirus-229E, -OC43, -NL63, and -HKU1 (Coronaviridae). Encyclopedia of Virology, 428–440. https://doi.org/10.1016/B978-0-12-809633-8.21501-X

[4] **Al-Salihi, K. A., & Khalaf, J. M.** (2021). The emerging SARS-CoV, MERS-CoV, and SARS-CoV-2: An insight into the viruses zoonotic aspects. Veterinary world, 14(1), 190–199. https://doi.org/10.14202/vetworld.2021.190-199

[5] **Cherry, J. D., & Krogstad, P.** (2004). SARS: the first pandemic of the 21st century. Pediatric research, 56(1), 1–5. https://doi.org/10.1203/01.PDR.0000129184.87042.FC

[6] **Memish, Z. A., Perlman, S., Van Kerkhove, M. D., & Zumla, A.** (2020). Middle East respiratory syndrome. Lancet (London, England), 395(10229), 1063–1077. https://doi.org/10.1016/S0140-6736(19)33221-0

[7] **Park S. E.** (2020). Epidemiology, virology, and clinical features of severe acute respiratory syndrome -coronavirus-2 (SARS-CoV-2; Coronavirus Disease-19). Clinical and experimental pediatrics, 63(4), 119–124. https://doi.org/10.3345/cep.2020.00493

[8] **Bhat, E. A., Khan, J., Sajjad, N., Ali, A., Aldakeel, F. M., Mateen, A., Alqahtani, M. S., & Syed, R.** (2021). SARS-CoV-2: Insight in genome structure, pathogenesis and viral receptor binding analysis - An updated review. International immunopharmacology, 95, 107493. https://doi.org/10.1016/j.intimp.2021.107493

[9] **Zhao, J., Qiu, J., Aryal, S., Hackett, J. L., & Wang, J.** (2020). The RNA Architecture of the SARS-CoV-2 3'-Untranslated Region. Viruses, 12(12), 1473. https://doi.org/10.3390/v12121473

[10] **Zhang, Y., Chai, Y., Hu, Z., Xu, Z., Li, M., Chen, X., Yang, C., & Liu, J.** (2022). Recent Progress on Rapid Lateral Flow Assay-Based Early Diagnosis of COVID-19. Frontiers in bioengineering and biotechnology, 10, 866368. https://doi.org/10.3389/fbioe.2022.866368

[11] **Huang, Y., Yang, C., Xu, X. F., Xu, W., & Liu, S. W.** (2020). Structural and functional properties of SARS-CoV-2 spike protein: potential antivirus drug development for COVID-19. Acta pharmacologica Sinica, 41(9), 1141–1149. https://doi.org/10.1038/s41401-020-0485-4

[12] **Lu, Y., Shen, F., He, W., Li, A., Li, M., Feng, X., Zheng, Y., & Pang, W.** (2023). HR121 targeting HR2 domain in S2 subunit of spike protein can serve as a broad-spectrum SARS-CoV-2 inhibitor via intranasal administration. Acta pharmaceutica Sinica. B, 13(8), 3339–3351. Advance online publication. https://doi.org/10.1016/j.apsb.2023.05.030

[13] **Khalid, Z., Khan, A. T., Alnajjar, R., Santali, E., & Shakoori, A. R.** (2022). In silico mutational analysis of ACE2 to check the susceptibility of lung cancer patients towards COVID-19. Scientific reports, 12(1), 7798. https://doi.org/10.1038/s41598-022-11805-5

[14] **Wu, W., Cheng, Y., Zhou, H., Sun, C., & Zhang, S.** (2023). The SARS-CoV-2 nucleocapsid protein: its role in the viral life cycle, structure and functions, and use as a potential target in the development of vaccines and diagnostics. Virology journal, 20(1), 6. https://doi.org/10.1186/s12985-023-01968-6

[15] **Morse, M., Sefcikova, J., Rouzina, I., Beuning, P. J., & Williams, M. C.** (2023). Structural domains of SARS-CoV-2 nucleocapsid protein coordinate to compact long nucleic acid substrates. Nucleic acids research, 51(1), 290–303. https://doi.org/10.1093/nar/gkac1179

[16] **Che, X. Y., Qiu, L. W., Pan, Y. X., Wen, K., Hao, W., Zhang, L. Y., ... & Yuen, K. Y.** (2004). Sensitive and specific monoclonal antibody-based capture enzyme immunoassay for detection of nucleocapsid antigen in sera from patients with severe acute respiratory syndrome. Journal of clinical microbiology, 42(6), 2629-2635.

[17] **Machado, B. A. S., Hodel, K. V. S., Barbosa-Júnior, V. G., Soares, M. B. P., & Badaró, R.** (2020). The Main Molecular and Serological Methods for Diagnosing COVID-19: An Overview Based on the Literature. Viruses, 13(1), 40. https://doi.org/10.3390/v13010040

[18] **Chan, J. F., Yip, C. C., To, K. K., Tang, T. H., Wong, S. C., Leung, K. H., Fung, A. Y., Ng, A. C., Zou, Z., Tsoi, H. W., Choi, G. K., Tam, A. R., Cheng, V. C., Chan, K. H., Tsang, O. T., & Yuen, K. Y.** (2020). Improved Molecular Diagnosis of COVID-19 by the Novel, Highly Sensitive and Specific COVID-19-RdRp/Hel Real-Time Reverse Transcription-PCR Assay Validated In Vitro and with Clinical Specimens. Journal of clinical microbiology, 58(5), e00310-20. https://doi.org/10.1128/JCM.00310-20

[19] **Kumar, P., Malik, Y. S., Ganesh, B., Rahangdale, S., Saurabh, S., Natesan, S., Srivastava, A., Sharun, K., Yatoo, M. I., Tiwari, R., Singh, R. K., & Dhama, K.** (2020). CRISPR-Cas System: An Approach With Potentials for COVID-19 Diagnosis and Therapeutics. Frontiers in cellular and infection microbiology, 10, 576875. https://doi.org/10.3389/fcimb.2020.576875

[20] **John, G., Sahajpal, N. S., Mondal, A. K., Ananth, S., Williams, C., Chaubey, A., Rojiani, A. M., & Kolhe, R.** (2021). Next-Generation Sequencing (NGS) in COVID-19: A Tool for SARS-CoV-2 Diagnosis, Monitoring New Strains and Phylodynamic Modeling in Molecular Epidemiology. Current issues in molecular biology, 43(2), 845–867. https://doi.org/10.3390/cimb43020061

[21] **Zambry, N. S., Obande, G. A., Khalid, M. F., Bustami, Y., Hamzah, H. H., Awang, M. S., Aziah, I., & Manaf, A. A.** (2022). Utilizing Electrochemical-Based Sensing

Approaches for the Detection of SARS-CoV-2 in Clinical Samples: A Review. Biosensors, 12(7), 473.

[22] **Kaloumenou, M., Skotadis, E., Lagopati, N., Efstathopoulos, E., & Tsoukalas, D.** (2022). Breath Analysis: A Promising Tool for Disease Diagnosis-The Role of Sensors. Sensors (Basel, Switzerland), 22(3), 1238. https://doi.org/10.3390/s22031238

[23] **Hammad, N. M., Saeed, M. A., Shaltout, S. W., Nofal, H. A., Nafae, R. M., Arslan, K., Tanoglu, A., Nechifor, M., Luca, C., Al-Kadhim, Z. H. A., Mosallem, A., & Amer, F. A.** (2022). RT- PCR testing of upper respiratory tract samples for diagnosis of SARS-CoV-2: Between justification and overestimation, a multi-center international study. Travel medicine and infectious disease, 48, 102334. https://doi.org/10.1016/j.tmaid.2022.102334

[24] **Rabe, B. A., & Cepko, C.** (2020). SARS-CoV-2 detection using isothermal amplification and a rapid, inexpensive protocol for sample inactivation and purification. Proceedings of the National Academy of Sciences of the United States of America, 117(39), 24450–24458. https://doi.org/10.1073/pnas.2011221117

[25] **Amellal, H., Assaid, N., Charoute, H., Akarid, K., Maaroufi, A., Ezzikouri, S., & Sarih, M.** (2023). Kinetics of specific anti-SARS-CoV-2 IgM, IgA, and IgG responses during the first 12 months after SARS-CoV-2 infection: A prospective longitudinal study. PloS one, 18(7), e0288557. https://doi.org/10.1371/journal.pone.0288557

[26] **Devi, M. J., Gaffar, S., & Hartati, Y. W.** (2022). A review post-vaccination SARS-CoV-2 serological test: Method and antibody titer response. Analytical biochemistry, 658, 114902. https://doi.org/10.1016/j.ab.2022.114902

[27] **Mohit, E., Rostami, Z., & Vahidi, H.** (2021). A comparative review of immunoassays for COVID-19 detection. Expert review of clinical immunology, 17(6), 573–599. https://doi.org/10.1080/1744666X.2021.1908886

[28] **Hernández-Pérez, J. M., Martín-González, E., & Pino-Yanes, M.** (2020). Strengths and weaknesses of the diagnostic tests for SARS-CoV-2 infection. Medicina clinica (English ed.), 155(10), 464–465. https://doi.org/10.1016/j.medcle.2020.05.025

[29] **Funari, R., Chu, K. Y., & Shen, A. Q.** (2020). Detection of antibodies against SARS-CoV-2 spike protein by gold nanospikes in an opto-microfluidic chip. Biosensors and Bioelectronics, 169, 112578.

[30] **Mojsoska, B., Larsen, S., Olsen, D. A., Madsen, J. S., Brandslund, I., & Alatraktchi, F. A. A.** (2021). Rapid SARS-CoV-2 detection using electrochemical immunosensor. Sensors, 21(2), 390.

[31] **Yari, P., Liang, S., Chugh, V. K., Rezaei, B., Mostufa, S., Krishna, V. D., ... & Wu, K.** (2023). Nanomaterial-Based Biosensors for SARS-CoV-2 and Future Epidemics. Analytical Chemistry.

[32] **Seo, G., Lee, G., Kim, M. J., Baek, S. H., Choi, M., Ku, K. B., Lee, C. S., Jun, S., Park, D., Kim, H. G., Kim, S. J., Lee, J. O., Kim, B. T., Park, E. C., & Kim, S. I.** (2020). Rapid Detection of COVID-19 Causative Virus (SARS-CoV-2) in Human Nasopharyngeal Swab Specimens Using Field-Effect Transistor-Based Biosensor. ACS nano, 14(4), 5135–5142. https://doi.org/10.1021/acsnano.0c02823

[33] **Dinnes, J., Sharma, P., Berhane, S., van Wyk, S. S., Nyaaba, N., Domen, J., Taylor, M., Cunningham, J., Davenport, C., Dittrich, S., Emperador, D., Hooft, L., Leeflang, M. M., McInnes, M. D., Spijker, R., Verbakel, J. Y., Takwoingi, Y., Taylor-Phillips, S., Van den Bruel, A., Deeks, J. J., … Cochrane COVID-19 Diagnostic Test Accuracy Group** (2022). Rapid, point-of-care antigen tests for diagnosis of SARS-CoV-2 infection. The Cochrane database of systematic reviews, 7(7), CD013705. https://doi.org/10.1002/14651858.CD013705.pub3

[34] **Singh, S., Wagh, V., & Chakole, S.** (2022). Identifying diagnosis of a pandemic COVID-19. Journal of Research in Medical and Dental Science, 10(7), 000-000.

[35] **Vealan, K., Joseph, N., Alimat, S., Karumbati, A. S., & Thilakavathy, K.** (2023). Lateral flow assay: a promising rapid point-of-care testing tool for infections and non-communicable diseases. Asian biomedicine : research, reviews and news, 17(6), 250–266. https://doi.org/10.2478/abm-2023-0068

[36] **Koczula, K. M., & Gallotta, A.** (2016). Lateral flow assays. Essays in biochemistry, 60(1), 111–120. https://doi.org/10.1042/EBC20150012

[37] **Kakkar, S., Gupta, P., Singh Yadav, S. P., Raj, D., Singh, G., Chauhan, S., Mishra, M. K., Martín-Ortega, E., Chiussi, S., & Kant, K.** (2024). Lateral flow assays: Progress and evolution of recent trends in point-of-care applications. Materials today. Bio, 28, 101188. https://doi.org/10.1016/j.mtbio.2024.101188

[38] **Bahadır, E. B., & Sezgintürk, M. K.** (2016). Lateral flow assays: Principles, designs and labels. TrAC Trends in Analytical Chemistry, 82, 286-306.

[39] **Wang, L., Wang, R., Wei, H., & Li, Y.** (2018). Selection of aptamers against pathogenic bacteria and their diagnostics application. World journal of microbiology & biotechnology, 34(10), 149. https://doi.org/10.1007/s11274-018-2528-2

[40] **Ince, B., & Sezgintürk, M. K.** (2022). Lateral flow assays for viruses diagnosis: Up-to-date technology and future prospects. Trends in analytical chemistry : TRAC, 157, 116725. https://doi.org/10.1016/j.trac.2022.116725

[41] **Hu, J., Choi, J. R., Wang, S., Gong, Y., Feng, S., Pingguan-Murphy, B., ... & Xu, F.** (2017). Multiple test zones for improved detection performance in lateral flow assays. Sensors and Actuators B: Chemical, 243, 484-488.

[42] **Mak, G. C., Cheng, P. K., Lau, S. S., Wong, K. K., Lau, C. S., Lam, E. T., Chan, R. C., & Tsang, D. N.** (2020). Evaluation of rapid antigen test for detection of SARS-CoV-2 virus. Journal of clinical virology : the official publication of the Pan American Society for Clinical Virology, 129, 104500. https://doi.org/10.1016/j.jcv.2020.104500

[43] **Kumar, V., Singh, J., Hasnain, S. E., & Sundar, D**. (2021). Possible Link between Higher Transmissibility of Alpha, Kappa and Delta Variants of SARS-CoV-2 and Increased Structural Stability of Its Spike Protein and hACE2 Affinity. International journal of molecular sciences, 22(17), 9131. https://doi.org/10.3390/ijms22179131

[44] **Dong, Y., Dai, T., Wei, Y., Zhang, L., Zheng, M., & Zhou, F.** (2020). A systematic review of SARS-CoV-2 vaccine candidates. Signal transduction and targeted therapy, 5(1), 237. https://doi.org/10.1038/s41392-020-00352-y

[45] **Liu, X., Yang, X., Wang, C., Liu, Q., Ding, Y., Xu, S., Wang, G., & Xiao, R.** (2024). A nanogap-enhanced SERS nanotag-based lateral flow assay for ultrasensitive and simultaneous monitoring of SARS-CoV-2 S and NP antigens. Mikrochimica acta, 191(2), 104. https://doi.org/10.1007/s00604-023-06126-x

[46] **Akbarzadeh, S., Khajehsharifi, H., & Hajihosseini, S.** (2022). Detection of Oxytetracycline Using an Electrochemical Label-Free Aptamer-Based Biosensor. Biosensors, 12(7), 468. https://doi.org/10.3390/bios12070468

[47] **Zhou, J., & Rossi, J.** (2017). Aptamers as targeted therapeutics: current potential and challenges. Nature reviews. Drug discovery, 16(3), 181–202. https://doi.org/10.1038/nrd.2016.199

[48] **Park, K. S., Park, T. I., Lee, J. E., Hwang, S. Y., Choi, A., & Pack, S. P.** (2024). Aptamers and Nanobodies as New Bioprobes for SARS-CoV-2 Diagnostic and Therapeutic System Applications. Biosensors, 14(3), 146. https://doi.org/10.3390/bios14030146

[49] **Thiviyanathan, V., & Gorenstein, D. G.** (2012). Aptamers and the next generation of diagnostic reagents. Proteomics. Clinical applications, 6(11-12), 563–573. https://doi.org/10.1002/prca.201200042

[50] **Dhar, P., Samarasinghe, R. M., & Shigdar, S.** (2020). Antibodies, Nanobodies, or Aptamers-Which Is Best for Deciphering the Proteomes of Non-Model Species?. International journal of molecular sciences, 21(7), 2485. https://doi.org/10.3390/ijms21072485

[51] **Gold L.** (2015). SELEX: How It Happened and Where It will Go. Journal of molecular evolution, 81(5-6), 140–143. https://doi.org/10.1007/s00239-015-9705-9

[52] **Xu, Y., Jiang, X., Zhou, Y., Ma, M., Wang, M., & Ying, B.** (2021). Systematic Evolution of Ligands by Exponential Enrichment Technologies and Aptamer-Based Applications: Recent Progress and Challenges in Precision Medicine of Infectious Diseases. Frontiers in bioengineering and biotechnology, 9, 704077. https://doi.org/10.3389/fbioe.2021.704077

[53] **Catuogno, S., & Esposito, C. L.** (2017). Aptamer Cell-Based Selection: Overview and Advances. Biomedicines, 5(3), 49. https://doi.org/10.3390/biomedicines5030049

[54] **Lan, J., Ge, J., Yu, J., Shan, S., Zhou, H., Fan, S., Zhang, Q., Shi, X., Wang, Q., Zhang, L., & Wang, X.** (2020). Structure of the SARS-CoV-2 spike receptor-binding domain bound to the ACE2 receptor. Nature, 581(7807), 215–220. https://doi.org/10.1038/s41586-020-2180-5

[55] **Poolsup, S., Zaripov, E., Hüttmann, N., Minic, Z., Artyushenko, P. V., Shchugoreva, I. A., Tomilin, F. N., Kichkailo, A. S., & Berezovski, M. V.** (2023). Discovery of DNA aptamers targeting SARS-CoV-2 nucleocapsid protein and protein-binding epitopes for label-free COVID-19 diagnostics. Molecular therapy. Nucleic acids, 31, 731–743. https://doi.org/10.1016/j.omtn.2023.02.010

[56] **Wan, Q., Liu, X., Zeng, Z., Chen, Z., Liu, Y., & Zu, Y.** (2020). Aptamer Cocktail to Detect Multiple Species of Mycoplasma in Cell Culture. International journal of molecular sciences, 21(11), 3784. https://doi.org/10.3390/ijms21113784

[57] **Kim, Y. S., Chung, J., Song, M. Y., Jurng, J., & Kim, B. C.** (2014). Aptamer cocktails: enhancement of sensing signals compared to single use of aptamers for detection of bacteria. Biosensors & bioelectronics, 54, 195–198. https://doi.org/10.1016/j.bios.2013.11.003

[58] **Chen, Z., Wu, Q., Chen, J., Ni, X., & Dai, J.** (2020). A DNA Aptamer Based Method for Detection of SARS-CoV-2 Nucleocapsid Protein. Virologica Sinica, 35(3), 351–354. https://doi.org/10.1007/s12250-020-00236-z

[59] **Song, Y., Song, J., Wei, X., Huang, M., Sun, M., Zhu, L., Lin, B., Shen, H., Zhu, Z., & Yang, C.** (2020). Discovery of Aptamers Targeting the Receptor-Binding Domain of the SARS-CoV-2 Spike Glycoprotein. Analytical chemistry, 92(14), 9895–9900. https://doi.org/10.1021/acs.analchem.0c01394

[60] **Çam, D., & Öktem, H. A.** (2017). Optimizations needed for lateral flow assay for rapid detection of pathogenic E. coli. Turkish journal of biology = Turk biyoloji dergisi, 41(6), 954–968. https://doi.org/10.3906/biy-1705-50

[61] **Omidfar, K., Riahi, F., & Kashanian, S.** (2023). Lateral Flow Assay: A Summary of Recent Progress for Improving Assay Performance. Biosensors, 13(9), 837. https://doi.org/10.3390/bios13090837

[62] **Abedi, N., Zeinoddini, M., & Shoushtari, M.** (2024). Optimized detection of Salmonella typhimurium using aptamer lateral flow assay. Biotechnology letters, 46(4), 583–592. https://doi.org/10.1007/s10529-024-03484-1

[63] **Chen, Z., Zhang, Z., Zhai, X., Li, Y., Lin, L., Zhao, H., Bian, L., Li, P., Yu, L., Wu, Y., & Lin, G.** (2020). Rapid and Sensitive Detection of anti-SARS-CoV-2 IgG, Using Lanthanide-Doped Nanoparticles-Based Lateral Flow Immunoassay. Analytical chemistry, 92(10), 7226–7231. https://doi.org/10.1021/acs.analchem.0c00784

[64] **Seo, H. B., & Gu, M. B.** (2017). Aptamer-based sandwich-type biosensors. Journal of biological engineering, 11, 11. https://doi.org/10.1186/s13036-017-0054-7

[65] **Chowdhury, P., Lawrance, R., Lu, Z.-Y., Lin, H.-C., & Chan, Y.-H.** (2024). Recent progress in dual/multi-modal detection modes for improving sensitivity and specificity of lateral flow immunoassays applied for point-of-care diagnostics. Trends in Analytical Chemistry, 177, 117798. https://doi.org/10.1016/j.trac.2024.117798

[66] **Trevethan R.** (2020). Response: Commentary: Sensitivity, Specificity, and Predictive Values: Foundations, Pliabilities, and Pitfalls in Research and Practice. Frontiers in public health, 7, 408. https://doi.org/10.3389/fpubh.2019.00408

CURRICULUM VITAE

Name and Surname: Elif GÜNDÜZ

EDUCATIONAL STATUS:

• **Bachelor of Science :** 2022, Inonu University, Faculty of Arts and Sciences, Department of Molecular Biology & Genetics (100% English), Malatya/Turkey

• **Master of Sceince :** 2024, Inonu University, Graduate School of Natural and Applied Sceinces, Department of Molecular Biology & Genetics (100% English), Malatya/Turkey

PUBLICATIONS

1. Çam Derin, D., Gültekin, E., Gündüz, E., & Otlu, B. (2024). Comparison of Six Aptamer-Aptamer Pairs on Rapid Detection of SARS-CoV-2 by Lateral Flow Assay. *Journal of AOAC International, 107*(3), 464–470.
2. Gündüz, E., & Çam Derin, D. İ. L. E. K. The Advantages of The Aptamer Usage in Lateral Flow Assays For Viral Detection.